이학박사 학위논문

Investigation on the surface tension of water nanodroplet using molecular dynamics simulations

분자동역학 시뮬레이션을 이용한 나노크기 물방울의 표면 장력에 대한 연구

2019년 8월

서울대학교 대학원

물리·천문학부

김 규 환

Investigation on the surface tension of water nanodroplet using molecular dynamics simulations

분자동역학 시뮬레이션을 이용한 나노크기 물방울의 표면 장력에 대한 연구

指導教授 諸元鎬

이 論文**을** 理學博士學位論文**으로** 提出**함**

2019年 **5** 月

서울大學校 大學院

物理·天文學部

金 奎 煥

金奎煥**의** 理學博士 學位論文**을** 認准**함**

2019年 **6** 月

委 員 長	박 건 식	印
副委員長	제 원 호	印
委 員	홍 승 훈	印
委 員	유 재 준	印
委 員	이 만 희	印

Investigation on the surface tension of water nanodroplet using molecular dynamics simulations

by

QHwan Kim, M.S.

Dissertation

Presented to the Faculty of the Graduate School of

Seoul National University

in Partial Fulfillment

of the Requirements

for the Degree of

Doctor of Philosophy

Seoul National University

August 2019

Abstract

Investigation on the surface tension of water nanodroplet using molecular dynamics simulations

QHwan Kim
Department of Physics and Astronomy
The Graduate School
Seoul National University

Surface tension controls ubiquitous phase transition phenomena such as condensation or evaporation of atmospheric liquid droplet. Especially, understanding of curved interface of critical nucleus, whose size is about 1 nm, is at the center of attention for overcoming nucleation energy barrier. Even a number of studies from the grand canonical Monte Carlo simulation, molecular dynamics simulation, density functional theory and to the nucleation experiments have been carried out, there is an insufficient understanding of whether the surface tension of nanodroplet is larger, smaller, or unchanged than the surface tension of macroscopic droplet. For accurate study, it is necessary to use methods which can give information of indivisual molecule because a single nanodroplet containes only tens or hundreds of molecules.

In this study, (1) the surface tension of small nanodroplets with a minimum size of 0.6 nm is obtained by using molecular dynamics simulations and pressure tensors derived from them. Molecular dynamics is suitable method for

studying such small systems because it considers the interaction of individual molecules and their trajectories. From the results, it is confirmed that when the nanodroplet size is smaller than 1 nm, the surface tension begins to decrease in size and decreases to 80% of the flat surface tension. (2) From the molecular dynamics results, we study the Tolman length and derive the accurate surface tension equation. This equation also explains why the previous surface tension equation, in particular Tolman's equation, cannot describe the droplet of less than 1 nm. This argument is confirmed with density functional theory of classical liquid at broad range of temperature. An additional analysis of the thermodynamic properties of water molecules shows that this feature of surface tension is due to the increase in the free energy of surface water molecules of the water droplet.

The surface tension study of nanodroplets exhibits that the interface of water nanodroplets has loosely connected hydrogen bond network, which attributes to the decreasing surface tension in nanoscale. Considering that the adsorption of molecules on the water-vapor interface can be achieved by disrupting water's hydrogen bonds, this observation suggests that the interaction between nanodroplet and other molecules can give results unpredicted in macroscopic scale. This future projects may extend applicability of the pure water nanodroplet to the studies of the aerosols or fine dusts.

Keywords : Surface Tension, Water Nanodroplet, Molecular Dynamics, Tolman Length, Gibbs-Tolman-Koenig-Buff Equation, Density Functional

Theory,

Student number : 2009-20398

Contents

List of Figures

Chapter 1

Introduction

Nanodroplets in clouds affect the transmission and reflectivity of sunlight and are critical to environmental and climate control [1–5]. In nature they can influence the transmittance and reflectance of clouds and consequently have an effect on the global radiation and temperature [4]. Therefore, understanding the mechanisms involved in nucleation of water nanodroplet in molecular scale has been strongly motivated.

In pure liquid without any other substances, nucleation process starts with the formation of a small embryo of liquid water clusters from supersaturated vapor phase, which will grow spontaneously only if its size exceeds a certain energy barrier. In classical nucleation theory (CNT), while formation of the volumetric energy of nanocluster is favorable, the excess free energy which is associated with formation of the continuous interface between the two phases is unfavorable one and plays a crucial role for determining the initial growth of

nanodroplet [6,7]. This unfavorable energy is expressed as a product of interface area and surface tension. Surface tension is defined as the change of free energy divided by change of area while volume of system is preserved. The surface tension in CNT formalism has been considered as the surface tension of the planar interface and it has been suffered from discrepancy between prediction and experiments [8]. In the case of water, this discrepancy exists along the 220 - 320 K temperature range [9–12].

A variety of different studies have been carried out to obtain accurate value of the surface tension of nanodroplet, from the grand canonical Monte Carlo simulation [13–16], molecular dynamics simulation [17–23], density functional theory [24,25] and to the experiments of nucleation of water nanodroplet [26], colloidal liquid [27], and concave water droplet [28,29]. However, there is still no consistency in the representation of the curvature dependence of interfacial properties in all these cases. In some studies of water droplets, for example, the tension is found to be a monotonically increasing function of the droplet size until the planar limit is reached, but even the qualitative trend is same, the cluster size where the tension essentially reaches the planar value differs from study to study.

The simplest and widely used scheme is to use the curvature expansion of the surface tension with the leading order correction, which is called Tolman's equation [30]. When R is the radius of surface tension, the surface tension is determined approximately $\gamma(R)/\gamma_0 = 1 - 2\delta(R)/R$, where γ_0 is the surface tension of a planar interface, δ is the Tolman length. Even this simple equation

is the good candidate for describing surface tension of nanodroplet, there is still no general consensus about the magnitude and sign of Tolman. Also, there is other important argument about necessity of quadratic or higher order term in Tolman's equation. Here, we use the molecular dynamics and density function theory to study the water and Lennard-Jones liquid nanodroplet. We calculate surface tension with developed pressure tensor method and show that surface tension of nanodroplet ~ 0.8 nm is smaller than planar surface tension. Study about Tolman length of nanodroplet gives precise equation of surface tension.

The study of surface tension of water nanodroplet by molecular dynamics simulation and density functional theory is examined in this thesis. The focus is primarily on the nanodroplet of pure water as the most universal of fluids. In chapter 2, we outline the theory behind the surface tension of planar and curved fluid interfaces. Tolman's equation and Gibbs-Tolman-Koenig-Buff equation are introduced. In chapter 3, we discuss algorithms used in molecular dynamics simulation. Integrator, thermostat, force field and water model for simulation of curved water-vapor interace are introduced. In chapter 4, we discuss the surface tension and relating properties of water nanodroplet with the result of MD simulation. MD simulation shows that surface tension of nanodroplet is smaller than that of planar interface at radius < 1.0 nm at 290 K. From the surface tension and Tolman length data, we derive the equation of surface tension as a extended version of Tolman's equaiton which can predict surface tension of water nanodroplet up to ~ 0.6 nm. And we analyze the properties in water molecules in nanodroplet to elucidate the origin of change of surface

tension on curved interface. Analysis of structure, thermodynamics, dynamics show that increasing Helmholtz free energy of interfacial water in nanodroplet induces the change of surface tension. In chapter 5, we introduce the density functional theory formalism for classical liquid obtain the surface tension and Tolman length data of Lennard-Jones liquid. Even the Lennard-Jones liquid is different with water, the surface tension of nanodroplet can be explained with the equation derived in chapter 4. It imples that there is general relation between curvature and surface tension of spherical system. Conclusions, future work and closing remarks are presented in Chapter 6.

Bibliography

[1] Baker, M. *Science* **276**, 1072-1078 (1997).

[2] Eastoe, J. et al. *Angew. Chem. Int. Ed.* **45**, 3675-3677 (2006).

[3] Wilhelmsen, O. et al. *Phys. Rev. E* **93**, 032801 (2016).

[4] Rosenfeld, D. *Science* **287**, 1793-1796 (2000).

[5] Kulmala, M. et al. *J. Aerosol Sci.* **35**, 143-176 (2004).

[6] Becker, R. & Doring, W. *Ann. Phys.* **24**, 719 (1935)

[7] Kalikmanov, V. *Nucleation Theory* (Spinger Netherlands, 2013)

[8] Iland, K., Wolk, J., Strey, R. & Kashchiev, D. *J. Chem. Phys.* **127**, 154506 (2007).

[9] Manka, A. A. et al. *J. Chem. Phys.* **132**, 244505 (2010).

[10] Brus, D., Zdimal, V. & Smolik, J. *J. Chem. Phys.* **129**, 174501 (2008).

[11] Brus, D., Zdimal, V. & Uchtmann, H. *J. Chem. Phys.* **131**, 074507 (2009).

[12] Wyslouzil, B. E. et al. *Phys. Chem. Chem. Phys.* **9**, 5353 (2007).

[13] Block, B. J. et al. *J. Chem. Phys.* **133**, 154702 (2010).

[14] Troster, A. & Binder, K. *Phys. Rev. Lett.* **107**, 265701 (2011).

[15] Das, S. K. & Binder, K. *Phys. Rev. Lett.* **107**, 235702 (2011).

[16] Troster, A. et al. *J. Chem. Phys.* **136**, 064709 (2012).

[17] Gloor, G. J., Jackson, G., Blas, F. J. & de Miguel, E. *J. Chem. Phys.* **123**, 134703 (2005).

[18] Errington, J. R. & Kofke, D. A. *J. Chem. Phys.* **127**, 174709 (2007).

[19] Sampayo, J. G., Malijevsky, A., Muller, E. A., de Miguel, E. & Jackson, G. *J. Chem. Phys.* **132**, 141101 (2010).

[20] Joswiak, M. N., Duff, N., Doherty, M. F. & Peters, B. *J. Phys. Chem. Lett.* **4**, 4267-4272 (2013).

[21] Factorovich, M. H., Molinero, V. & Scherlis, D. A. *J. Am. Chem. Soc.* **136**, 4508-4514 (2014).

[22] Lau, G. V. et al *J. Chem. Phys.* **142**, 114701 (2015).

[23] Joswiak, M. N., Do, R., Doherty, M. F. & Peters, B. *J. Chem. Phys.* **145**, 204703 (2016).

[24] Koga, K., Zeng, X. C. & Shchekin, A. K. *J. Chem. Phys.* **109**, 4063 (1998).

[25] Malijevsky, A. & Jackson, G. *J. Phys.: Condens. Matter* **24**, 464121 (2012).

[26] Bruot, N. & Caupin, F. *Phys. Rev. Lett.* **116**, 056102 (2016).

[27] Nguyen, V. D., Schoemaker, F. C., Blokhuis, E. M. & Schall, P. *Phys. Rev. Lett.* **121**, 246102 (2018).

[28] Kim, S., Kim, D., Kim. J., An. S & Jhe. W. *Phys. Rev. X* **8**, 041046 (2018).

[29] Kwon, S., Kim, B., An, S., Lee, W., Kwak, H. & Jhe. W. *Sci. Rep* **8**, 8462 (2018).

[30] Tolman, R. C. *J. Chem. Phys.* **17** 333 (1949).

Chapter 2

Theoretical Overview

2.1 Introduction

In this chapter, we introduce the theory about the surface tension of planar and curved interfaces. The thermodynamics of curved interface results the derivation of Tolman's equation [1] which explains surface tension of nanodroplet with lowest order. We also provide review of the literature about simulation methods for obtaining the surface tension of planar and curved vapor-water interfaces, which is the main goal of this thesis.

2.2 Surface tension

This section deals with interfaces between two different phases and the resulting thermodynamic definition of the surface tension. Starting point of investigation

of bulk liquid system with thermodynamics is fundamental thermodynamic relation given as [2]

$$\mathrm{d}F = -S\mathrm{d}T - P\mathrm{d}V + \sum_{i=1}^{j} \mu_i \mathrm{d}N_i, \tag{2.1}$$

where F is the Helmholtz free energy, T is the temperature, P is the pressure, S is the entropy, V is the volume, j is the number of components, μ_i is the chemical potential of component i and N_i is the number of particles of component i in the system. If two different bulk systems meet and does not mix each other, the phases are separated and interface between them is created (Fig. 2.1). The interface brings an additional variable of area A where surface energy is stored. To take out the surface energy, let us assum that one can vary the area infinitesimally from A to $A + \mathrm{d}A$ while keeping volume under isothermal condition. Then Helmholtz free energy changes from F to $F + \mathrm{d}F$. This means that $\mathrm{d}F$ is proportional to $\mathrm{d}A$ and the constant of proportionality taken as $\mathrm{d}F/\mathrm{d}A$ in the limit $\mathrm{A} \to 0$, is called the surface tension (or, more generally, the surface free energy) γ. The differential change in Helmholtz free energy when the area is included can be rewritten as

$$\mathrm{d}F = -S\mathrm{d}T - P\mathrm{d}V + \sum_{i} \mu \mathrm{d}N_i + \gamma \mathrm{d}A, \tag{2.2}$$

and the surface tension can then be expressed as

$$\gamma = \left(\frac{\partial F}{\partial A}\right)_{N_i,V,T} = \lim_{\Delta A \to 0} \left(\frac{\Delta F}{\Delta A}\right)_{N_i,V,T} \tag{2.3}$$

where the partial derivative (left hand side) is equivalent to the finite difference version (right hand side) in the limit $\Delta A \to 0$. The surface tension γ can

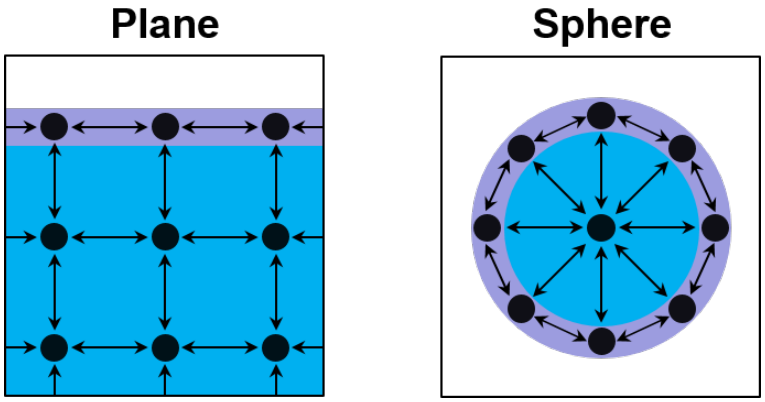

Figure 2.1: Schematic of planar and spherical system. Spheres and arrows denote liquid atoms and their interactions respectively. The interface of system is emphasized with different color.

be considered as the change in free energy for an infinitesimal change in the interfacial area, i.e., a measure of the cost in free energy associated with changing the interfacial area. While considering the interfacial energy is related with the interaction of interfacial molecules, we can also consider surface tension of nanoscale droplet. Figure 2.1 shows schematic of spherical droplet whose size is comparable of molecular diameter. In this case, the configuration of interfacial molecules cannot be same as that of planar interface because system geometry affects configuration. As a basic concept, we can assume that surface tension of nanodroplet is different with that of plane interface.

2.3 Simulation methods for obtaining the surface tension

For the determination of the surface tension of interfaces using by Monte Carlo (MC) or molecular dynamics (MD) simulation, three different methods has been used. The first (and most common) approach is compute surface tension by using the components of the pressure tensor [3–5]. In the case of a planar interface the surface tension γ can be obtained from the condition of mechanical equilibrium as an integral in the difference of the normal $P_n(z)$ and tangential $P_t(z)$ components of the pressure tensor across the interface [2] as

$$\gamma = \int \left[P_n(z) - P_t(z)\right], \tag{2.4}$$

where z denotes the direction normal to the interface.

The second approaches follows a thermodynamic definition of surface tension and calculates the difference in free energy for systems in macrostates with different interfacial areas [6, 7]. In this so-called test-area method [6] the free-energy difference between a reference and a perturbed system of different area can be expressed as a ratio of their partition functions, which reduces to a difference of configurational energys for isothermal perturbations. A thermodynamic expression for the surface tension can then be written as

$$\gamma = \left(\frac{\partial F}{\partial A}\right)_{N,V,T} = \lim_{\Delta A \to 0} \frac{1}{\Delta A}\left[\langle \Delta U \rangle - \frac{1}{2k_{\mathrm{B}}T}\left(\left\langle \Delta U^2 \right\rangle - \langle \Delta U \rangle^2\right)\right] + O\left(\Delta U^3\right), \tag{2.5}$$

where ΔA is the difference of surface area, ΔU the difference in configurational

energy between the perturbed and reference systems, and k_{B} is the Boltzmann constant. The angled brackets denote a canonical average in the ensemble associated with the reference unperturbed (subscript 0) system.

The third method uses the grand canonical ensemble (constant μ_i, V, T) [8–11]. This approach determines the surface free energy of an interfacial system by obtaining the Landau free-energy barrier between the coexisting states during a simulation. The surface tension of an infinite system can not be computed and is estimated by extrapolation from results of curved interface.

The surface tension of the planar vapor-liquid interface of water has been studied extensively by computer simulation (e.g., see references [12–15]). In MD simulation, procedure typically involves placing a thick slab of liquid in contact with vapor and computing the surface tension using the pressure tensor. The value of the vapor-liquid surface tension reported in these literatures vary due to several factors such as the system size, simulation legth, parameter of simulation, and choice of water model.

2.4 Thermodynamics of curved interfaces

In the nucleation of a liquid from a supersaturated vapor, one should know properties of spherical liquid nanodroplets. This is because when the clusters are created, they are composed of few tens or hundreds of molecules and the surface minimizes itself to minimize the unfavored energy during nucleation process and forms spherical nanodroplet. The theoretical investigation of the

thermodynamics of curved interfaces is a greater challenge than that of planar interfaces [16, 17]. The study starts from seminal macroscopic mechanical description of Young [18] at the nineteenth century, followed by the Tolman [1] with his popular Tolman's equation.

2.4.1 The Young-Laplace equation

Young and Laplace noted that the pressure difference between the inside and outside of a spherical liquid drop in equilibrium is proportional to the product of surface tension and inverse radius:

$$P_{\mathrm{l}} - P_{\mathrm{v}} = \frac{2\gamma}{R}, \tag{2.6}$$

where P_{l} and P_{v} are the pressures of the liquid inside and the vapor outside the drop, respectively, and R is the radius of the drop. This relation can be derived by considering a curved interface between two phases α and β in equilibrium. The thermodynamic relation for this system is obtained by rewritting Eq. (2.2) as

$$\mathrm{d}U = T\mathrm{d}S - (P_\alpha \mathrm{d}V_\alpha + P_\beta \mathrm{d}V_\beta) + \sum_i \mu_i \left(\mathrm{d}N_{\alpha,i} + \mathrm{d}N_{\beta,i}\right) + \gamma \mathrm{d}A. \tag{2.7}$$

If we change radius of curvature from R to $R + \Delta R$ while keeping the total volume, entropy and particle number, then we can get following relations,

$$\mathrm{d}V_\beta = -\mathrm{d}V_\alpha = 4\pi R^2 \mathrm{d}R \tag{2.8}$$

$$\mathrm{d}A = 8\pi R \mathrm{d}R. \tag{2.9}$$

Note that other thermodynamic quantities are zero at isothermal condition. Substituting Eqs. (2.8) and (2.9) into Eq. (2.7) gives the Young-Laplace equation as

$$P_\beta - P_\alpha = \frac{2\gamma}{R}, \tag{2.10}$$

In the case of a liquid drop in vapor, the phases α and β correspond to the vapor and liquid phases respectively. In the case of a liquid bubble or capillary bridge, the pressure difference becomes negative and they are reversed.

2.5 Curvature corrections to the surface tension

Tolman [1] used the thermodynamic framework introduced by Gibbs [19] and derive an expression for the dependence of the tension γ on the drop size:

$$\gamma = \gamma_0 \left(1 + \frac{2\delta_0}{R_s}\right)^{-1} \tag{2.11}$$

where R_s is the radius of the spherical surface of tension (defined as the surface where the Young-Laplace Eq. (2.10) holds exactly [2, 19]), and δ_0 is the so-called Tolman length (in the planar limit). The Tolman's equation is commonly expressed as a polynomial series of the curvature (inverse radius),

$$\gamma = \gamma_0 \left(1 - \frac{2\delta_0}{R_\mathrm{s}} + \cdots\right). \tag{2.12}$$

Though the physical significance of terms beyond leading order have been brought into question [2]. In any case, the magnitude of the Tolman length

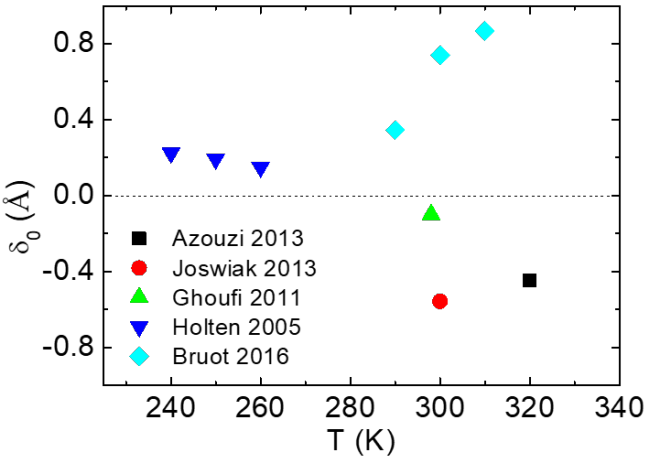

Figure 2.2: Tolman length determined from various studies.

has been shown to be small and difficult to determine even for the simplest of fluids [20–22]. In Fig. 2.2, we plot the some results of determination of Tolman length from experiments [23–25] and simulations [26, 27]. It clearly shows that there is no general consensus about sign and magnitude of Tolman length.

2.5.1 Derivation of Tolman's equation

We start with two different definitions of surface of nanodroplet. Because radius and surface is zero-thickness definition mathematically, there are infinite ways to define radius of nanodroplet. Here we use two most important definition of radius, equimolar radius (R_e) and radius of surface tension (R_s). Imagine that the liquid nanodroplet is formed from supersaturated vapor. Then number of

molecules in droplet, ΔN is defined with equimolar radius as

$$\Delta N = N - \rho_{\mathrm{v}} V = \Delta\rho \frac{4}{3}\pi R_{\mathrm{e}}^3. \tag{2.13}$$

And radius of surface tension denotes location where surface tension is defined and determined from Laplace equation as

$$\Delta P = \frac{2\gamma(R_{\mathrm{s}})}{R_s}. \tag{2.14}$$

We will express the grand potential difference for nucleating nanodroplet from vapor, $\Delta\Omega$, with two definitions. At first, with R_{s}, the energy cost is represented by sum of favored volume energy and unfavored surface energy as

$$\Delta\Omega = -\frac{4}{3}\pi R_{\mathrm{s}}^3 \Delta P + 4\pi R_{\mathrm{s}}^2 \gamma(R_{\mathrm{s}}), \tag{2.15}$$

and its derivative is expressed as

$$\mathrm{d}\Delta\Omega = -\frac{4}{3}\pi R_{\mathrm{s}}^3 \mathrm{d}\Delta P + 4\pi R_{\mathrm{s}}^2 \mathrm{d}\gamma(R_{\mathrm{s}}). \tag{2.16}$$

Note that other two terms are cancelled with Laplace equation. The grand potential also can be expressed as the product of number of molecules and chemical potential as

$$\mathrm{d}\Delta\Omega|_{T,V} = -N\mathrm{d}\mu = -\frac{4}{3}\pi R_{\mathrm{e}}^3 \mathrm{d}\Delta P. \tag{2.17}$$

Equating Eq. (2.16), Eq. (2.17) and insert relation $\delta = R_{\mathrm{e}} - R_{\mathrm{s}}$ gives

$$-\delta\left(1 + \frac{\delta}{R_{\mathrm{s}}} + \frac{\delta^2}{3R_{\mathrm{s}}^2}\right)\mathrm{d}\Delta P = \mathrm{d}\gamma. \tag{2.18}$$

$\mathrm{d}\Delta P$ is replaced with Laplace equation and one can get equation relating surface tension and radius of surface tension as

$$\frac{\mathrm{dln}\gamma}{\mathrm{dln}R_\mathrm{s}} = \frac{\frac{2\delta}{R_\mathrm{s}}\left[1+\frac{\delta}{R_\mathrm{s}}+\frac{1}{3}\left(\frac{\delta}{R_\mathrm{s}}\right)^2\right]}{1+\frac{2\delta}{R_\mathrm{s}}\left[1+\frac{\delta}{R_\mathrm{s}}+\frac{1}{3}\left(\frac{\delta}{R_\mathrm{s}}\right)^2\right]}. \tag{2.19}$$

This equation is induced by Tolman and is now called Gibbs-Tolman-Koenig-Buff (GTKB) equation [2,19,28,29]. Equation (2.11) is obtained if one assumes $\delta = \delta_0$ and neglects high order of $1/R_\mathrm{s}$.

2.6 Simulation of water nanodroplet

In this section we introduce the studies of determination of surface tension of water nanodroplet using molecular simulation. Samsonov et al. [30] used the Stockmayer potential parameterized to represent water. The surface tension determined at 300 K was found to be a monotonically increasing function of the equimolar radius, starting from $\gamma \sim 20$ mN/m for $R \sim 0.2$ nm and reaching the asymptotic planar value at $R = 1$ nm. Ghoufi and Malfreyt [27] performed mesoscale Monte Carlo simulations of water nanodroplets with a DPD (dissipative particle dynamics) model. They calculate the pressure tensor components with energy perturbation method and obtain a monotonic behavior for the curvature dependence of the surface tension. Joswiak et al. [26] employed the mitosis method to evaluate the free energy associated with separating a liquid drop into a pair of smaller drops to estimate the surface tenison of water nanodroplets of the TIP4P/2005 model. Their results show that the surface tension at 300

K increases continuously from the planar limit of $\gamma_0 = 65.6$ mN/m to $\gamma = 77$ mN/m on decreasing the size of the nanodroplet to a radius of $R \sim 0.6$ nm. A similar increase in the interfacial tension of the TIP4P model by more than 10 mN/m from the planar limit on decreasing the radius to $R = 0.7$ nm was obtained by Homman et al. [31] using the Laplace relation with a determination of the surface of tension R_s. On the other hand, in their analysis of the vapor pressure of water nanodroplet, Factorovich et al. [32] have demonstrated that surface tension of nanodroplet can be smaller than that of planar tension at $R \sim 0.6$ nm. Lau et al. [33] uses the similar method with Joswiak et al. [26] with careful consideration of statistical dynamics and obtain decreasing surface tension.

2.7 Conclusion

This chapter introduces broad range of previous studies about surface tension of water nanodroplets and they show controversial results, which is worthy of further consideration.

Bibliography

[1] Tolman, R. C. *J. Chem. Phys.* **17**, 333 (1949).

[2] Rowlinson, J. S. & Widom, B. *Molecular Theory of Capillarity* (Oxford Univ., Oxford, 1982).

[3] Kirkwood, J. G. & Buff, F. P. *J. Chem. Phys.* **17**, 338 (1949).

[4] Ikeshoji, T., Hafskjold, B. & Furuholt, H. *Mol. Sim.* **2**, 101-109 (2003).

[5] Vrabec, J., Kedia, G. K., Fuchs, G. & Hasse, H. *Mol. Phys.* **104**, 1509 (2006).

[6] Gloor, G. J., Jackson, G., Blas, F. J. & De Miguel, E. *J. Chem. Phys.* **123**, 134703 (2005).

[7] Errington, J. R. & Kofke, D. A. *J. Chem. Phys.* **127**, 174709 (2007).

[8] Binder, K. *Phys. Rev. A* **25**, 1699 (1982).

[9] Troster, A. & Binder, K. *Phys. Rev. Lett.* **107**, 265701 (2011).

[10] Das, S. K. & Binder, K. *Phys. Rev. Lett.* **107**, 235702 (2011).

[11] Troster, A. et al. *J. Chem. Phys.* **136**, 064709 (2012).

[12] Matsumoto, M., Takaoka, Y. & Kataoka, Y. **98**, 1464 (1993).

[13] Yasuoka, K. & Matsumoto, M. **109**, 8463 (1998).

[14] Vega, C. & De Miguel, E. *J. Chem. Phys.* **126**, 154707 (2007).

[15] Ghoufi, A. & Malfreyt, P. *Phys. Rev. E* **83**, 051601 (2011).

[16] Henderson, J. R. *Statistical Mechanics of Spherical Interfaces* (Wiley, New York, 1986).

[17] Malijevsky, A. & Jackson, G. *J. Phys.: Condens. Matter* **24**, 464121 (2012).

[18] Young, T. *Phil. Trans.* **95**, 65 (1805).

[19] Gibbs, J. W., Bumstead, H. A. & van Name, R. G. *Scientific Papers of J. Willard Gibbs: Thermodynamics* (Longmans and Green, New York).

[20] Blokhuis, E. M. & Bedeaux, D. *J. Chem. Phys.* **97**, 3576 (1992).

[21] Lei, Y. A., Bykov, T., Yoo, S. & Zeng, X. C. *J. Am. Chem. Soc.* **127**, 15346 (2005).

[22] Horsch, M et al. *Phys. Rev. E* **85**, 031605 (2012).

[23] Azouzi, M. E. M et al. *Nat. Phys.* **9**, 38 (2013).

[24] Holten, M. et al. *J. Chem. Phys.* **123**, 104505 (2005).

[25] Bruot, N. & Caupin, F. *Phys. Rev. Lett.* **116**, 056102 (2016).

[26] Joswiak, M. N., Duff, N., Doherty, M. F. & Peters, B. *J. Phys. Chem. Lett.* **4**, 4267 (2013).

[27] Ghoufi, A. & Malfreyt, P. *J. Chem. Phys.* **135**, 104105 (2011).

[28] Koenig, F. O. *J. Chem. Phys.* **18**, 449 (1950).

[29] Buff, F. P. *J. Chem. Phys.* **19**, 1591 (1951).

[30] Samsonov, V., Bazulev, A. & Sdobnyakov, N. Y. *Dokl. Phys. Chem.* **389**, 83 (2003).

[31] Homman, A. A. et al. *J. Chem. Phys.* **140**, 034110 (2014).

[32] Factorovich, M. H., Molinero, V. & Scherlis, D. A. *J. Am. Chem. Soc.* **136**, 4508 (2014).

[33] Lau. G. V. et al. *J. Chem. Phys.* **143**, 244709 (2015).

Chapter 3

Molecular Dynamics Simulation

3.1 Introduction

In this section we introduce about aspects of molecular dynamics (MD) simulation. MD gives a huge advantage about the possibility to gain a information of statistical system with a single molecular level. Not only statistical physics of bulk system, in broad range of study and application, there is necessities about information of system of few tens of molecules in nanosystem only can be undersood on a molecular level. The aim of molecular dynamics simulations is to calculate the equation of motion of each molecules with governing equation and obtain the trajectories to recover phase space of system [1]. Not only governing equation, another algorithms such as thermostat, barostat, choice of force field and molecule model should be considered to correctly simulate the real world into the numerical world. From this perspective, molecular dynamics simula-

tions can be seen as a bridge between the microscopic molecular level world of statistical mechanics and the macroscopic thermodynamic world.

3.2 Governing equation

In molecular dynamics simulation, we get the time trajectories of every particles in the system starting from the initial positions and velocities by solving governing equations of motion. In classical mechanics, the total force acting $\vec{F}$ on each atom in the system can be found by the negative gradient of the potential energy $U(r)$ between two atoms separated by a distance r as,

$$\vec{F} = -\nabla U(\vec{r}). \tag{3.1}$$

This Newton's equations of motion are calculated numerically. In the preparation step of simulation, the initial configuration of the components in the simulation system is known, and then Eq. (3.1) is used to calculate the total force acting on each atom in the system and their accelerations. This gives a time evolution of the system, and the position and momentum of each atom is updated each time step.

3.3 Integration of the equations of motion

Newton's second law of single particle can be stated as,

$$\vec{F}_i = m_i \vec{a}_i = \frac{\mathrm{d}^2 \vec{r}_{\mathrm{i}}}{\mathrm{dt}^2}, \tag{3.2}$$

where $\vec{F}$ is the total force exerted on particle i, m_i is the mass, $\vec{a}_i$ is the acceleration, $\vec{r}_i$ is the position vector and t is the time.

By combining Eqs. (3.1) and (3.2), the acceleration of each particle can be calculated each time frame. In a molecular dynamics simulation, it is necessary to solve the Newton's equation with integration algorithm to advance the system in time. In this thesis we use the leap-frog integrator to time integrate the simulations [2].

The leap-frog algorithm uses positions $\vec{r}$ at time t and velocities $\vec{v}$ at time $t-1/2\Delta t$, where Δt is the timestep between two neighboring configurations. It updates positions and velocities using the forces $\vec{F}(t)$ determined by the positions at time t using these relations as

$$\vec{v}(t+\frac{1}{2}\Delta t) = \vec{v}(t-\frac{1}{2}\Delta t) + \frac{\Delta t}{m}\vec{F}(t) \tag{3.3}$$

$$\vec{r}(t+\Delta t) = \vec{r}(t) + \Delta t\,\vec{v}(t+\frac{1}{2}\Delta t). \tag{3.4}$$

From these two equations, we can update positions as

$$\vec{r}(t+\Delta t) = 2\vec{r}(t) - \vec{r}(t-\Delta t) + \frac{1}{m}\vec{F}(t)\Delta t^2 + O\left(\Delta t^4\right). \tag{3.5}$$

This is of third order algorithm in $\vec{r}$ and time-reversible. The timestep Δt is often used with 1 - 2 fs in molecular dynamics simulations with water molecules. Note that this algorithm is correct for NVE ensemble and when thermostat, barostat or constraints are applied can be modified, which are decribed below.

3.4 Force fields

Without force field, molecular dynamics system is just the collection of radom billiard balls and rods connecting them. With good force fields, MD results well reproduce the experiments. Force fields provide the input parameters used by the governing equations of motion to calculate the positions and velocities of the atoms. Each atom in the system are described by a set of force field parameters. There exist many force fields and choosing the correct one for the simulation system and conditions can be critical for the results. The total potential energy U_{tot} is often divided into two groups as

$$U_{\text{tot}} = U_{\text{bonded}} + U_{\text{non-bonded}}, \tag{3.6}$$

where U_{bonded} represents the bonding potential between two (bond), three (angle), four(dihedrals, impropers) atoms linked with covalent bonds. Hoever, for various force fields of water molecules, we use TIP4P/2005 model [3] including constraint algorithm for fixing the bond length and angle between oxygen and hydrogen molecules. Thus, in this thesis $U_{\text{bonded}} = 0$ and only non-bonded potential will be considered.

The non-bonded interactions are both intra- and intermolecular. For example, if we use large molecules such as protein, non-bonded interactions exist between atoms in different residues in protein. The non-bonded interactions can be divided into two types: long-range and short-range. The long-range interactions are electrostatic forces, generally described by Coulomb's law. The short-range interactions are vdW (van der Waals) interactions and are typically

described by a Lennard-Jones potential. The non-bonded interactions can be expressed as,

$$U_{\text{non-bonded}} = U_{\text{C}} + U_{\text{vdW}}. \tag{3.7}$$

Here we use the Lennard-Jones 12-6 potential as the short-range potential [4], which is most common short-range potential model,

$$U_{\text{vdW}}(r) = U_{\text{LJ}}(r) = 4\epsilon \left[\left(\frac{\sigma}{r}\right)^{12} - \left(\frac{\sigma}{r}\right)^{6} \right], \tag{3.8}$$

where ϵ is the well depth of the potential and σ is the van der Waal radius. Variation of ϵ and σ for different atom species makes the Lennard-Jones potential unique for each component of a simulation system. The electrostatic non-bonded interactions act on long-range and are considered as strong forces. For many force fields, the partial charges assigned to each atom. The partial charge of each atoms are located at the center of each atoms, hence, electrostatic interactions can also be called simple point charge interactions. By reducing the electrostatic interactions to simple point charge interactions, Coulomb's law can be used to calculate the electrostatic forces between two atoms. The Coulomb's law can be expressed as

$$U_{\text{C}}(r_{ij}) = \frac{1}{4\pi\varepsilon_0} \frac{q_i q_j}{\varepsilon_r r_{ij}}, \tag{3.9}$$

where q_i and q_j are the partial simple point charges for atoms i and j, r_{ij} is the absolute distance vector between the two atoms, ε_0 is the permittivity of vacuum and ε_r is the relative permittivity. The value of paramters for force fields are chosen by fitting with experimental data or approximated with advanced quantum mechanics calculations [5, 6].

Because Coulomb interaction is long-range, calculating it with long cut-offs is heavy task for computer. With small cut-off ($\sim$ 1.5 nm), there are some algorithms for fast calculation of long-range part of Coulomb interaction as correction such as reaction field method [7], Ewald summation method [8], or partical mesh Ewald method [9]. However, in this thesis, we study about nanodroplet with finite size and long-range potential of this system can be obtained with long cut-offs ($\sim$ 10 nm), which is smaller than the size of nanodroplet. So in this chapter we omit introduction about these correction algorithms.

3.5 Periodic boundary conditions

In molecular dynamics, system is considered as the box with finite volume. If the wall of system is not blocked, the atoms can escape the box and can induce the error. However, if we block the box with some artifical walls, the basic goal of MD simulation about reproducing statistical ensemble can be violated. To account for this controversy, periodic boundary conditions (PBC) are applied to the simulation system to make it a periodic system. Figure 3.1 illustrates the concept of periodic boundary conditions. In Fig. 3.1, the system box is drawn in 2-dimensions for simplicity. If the system is 3-dimension, 26 periodic images are necessary. The original box is the box in the middle with nanodroplet with bold color. In a 2-dimensional space like this, when the periodic boundary conditions are applied correctly to the simulations system, there will be a copy of the original box on each side of the original box. So, in this example 8 images

are created and they have the exact same movement as the neighbouring box. When an atom exits and enters into the neighbouring box, a copy of that atom from neighbor image enter into the box where it came from. Thus, by applying periodic boundary conditions to the system, it is possible to maintain the number of molecules of the system constant with time. It also makes it possible to simulate an infinite large bulk system in the periodic directions, even with small amounts of atoms.

3.6 Temperature control

In molecular dynamics simulation, the temperature is defined as the average kinetic energy of molecules as

$$\langle E_k \rangle = \frac{1}{2} \sum_i m_i \left\langle v_i^2 \right\rangle = \frac{3}{2} k_{\mathrm{B}} T, \tag{3.10}$$

where $\langle E_k \rangle$ is the average kinetic energy, m_i is the mass of particle i, v_i is the velocity of particle i, k_{B} is the Boltzmann constant and T is the temperature. The most natural ensemble in molecular dynamics simulations would be to use the microcanonical (NVE) ensemble due to energy conservation and the Newton's equations of motion. But most experiments are carried out under the conditions of constant temperature or pressure, not constant energy. When the canonical ensemble (NVT) is used in molecular dynamics simulations, it is necessary to use a thermostat to keep the temperature constant. There exist many computational algorithms for that purpose. There are three popular examples are: the Nose-Hoover thermostat [10, 11], the Berendsen thermostat [12]

and the Andersen thermostat [13]. In this thesis, we deal with NVT ensemble with Nose-Hoover thermostat because it gives correct distribution of velocities and dynamical properties [14]. The goal with a thermostat is to keep the average temperature of the system constant while preserving Maxwell-Boltzmann velocity distribution of molecules. The system Hamiltonian is extended by introducing a thermal reservoir and a friction term in the equations of motion. The friction force is proportional to the product of each particle's velocity and a friction parameter, ζ. This friction parameter is a fully dynamic quantity with its own momentum (p_ζ) and equation of motion; the time derivative is calculated from the difference between the current kinetic energy and the reference temperature. In this formulation, the equations of motion of particles in Eq. (3.2) are replaced by,

$$\frac{\mathrm{d}^2\vec{r}_{\mathrm{i}}}{\mathrm{dt}^2} = \frac{\vec{F}_i}{m_i} - \frac{p_\zeta}{Q}\frac{\mathrm{d}\vec{r}_{\mathrm{i}}}{\mathrm{dt}}, \tag{3.11}$$

where the equation of motion for the heat bath parameter ζ is given as,

$$\frac{\mathrm{dp}_\zeta}{\mathrm{dt}} = (T - T_0). \tag{3.12}$$

The reference temperature is denoted T_0, while T is the current instantaneous temperature of the system which is determined by Eq. (3.10). The strength of the coupling is determined by the constant Q in combination with the reference temperature.

The conserved quantity for the Nose-Hoover equations of motion is not the total energy, but rather

$$H = \sum_{i=1}^{N} \frac{\vec{p}_i}{2m_i} + U(\vec{r}_N) + \frac{p_\zeta^2}{2Q} + N_f k_{\mathrm{B}} T\zeta, \tag{3.13}$$

where N_f is the total number of degrees of freedom.

3.7 Water models

In particular, water is important species in MD simulation because it is almost always included in biology, chemistry related system. The water models provide the specially tailored force fields for water molecules. There are plenty of water models have been published in the literature so far. Most of these models are consisted of three or four atoms with rigid bonding and angle because this simple model can be used in large systems ($> 10^4$ molecules) or for long simulation periods (> 10 ns). If we want to use more complex models, we should sacrifice these benefits, but we can obtain more accurate result, such as spectrum data (generally obtained from *ab initio* MD) [15].

In this thesis, we use TIP4P/2005 water model [3]. TIP4P/2005 is one of famous water model used nowadays. This is composed of one oxygen atom and two hydrogen atoms and one virtual atom with zero mass. The virtual atom only carries charges. The schematic and force field of TIP4P/2005 model is shown in Fig. 3.2 and Table 3.1. It is used in broad range of simulation study such as phase transition in nanoconfined system [16], phase properties of supercooled water [17], prediction of new metastable water phase [18], interface of water-vapor [19]. We choose this model because it correctly predicts the experiments of bulk liquid water [3].

There are lots of famous other water models. For three-site model, TIP3P

Table 3.1: Parameters of TIP4P/2005 water model.

r_{OH}(nm)	θ_{HOH} (deg.)	r_{OM} (nm)	σ (nm)	ϵ (kJ/mol)	q_O (e)	q_H (e)	q_M (e)
0.09572	104.52	0.01546	0.31589	0.77490	0	0.5564	-1.1128

[20] and SPC/E [21] model are widely used. For five-site model, TIP5P model is famous [22]. There is also the polarized SWM4-NDP model [23] similar to the TIP4P model in structure, except for the Drude particle attached to the oxygen site through a harmonic spring.

3.8 Conclusion

In this section, we introduce some core algorithms for running MD simulation and force fields of water molecule used in this thesis. Even these algorithms are complex to implement and time-consuming process, there are many free and fast software of MD simulation such as GROMACS [24], LAMMPS [25], AMBER [26], NAMD [27], DL-POLY [28]. With these open-source softwares, anybody can carry out MD simulation of diverse systems in linux system.

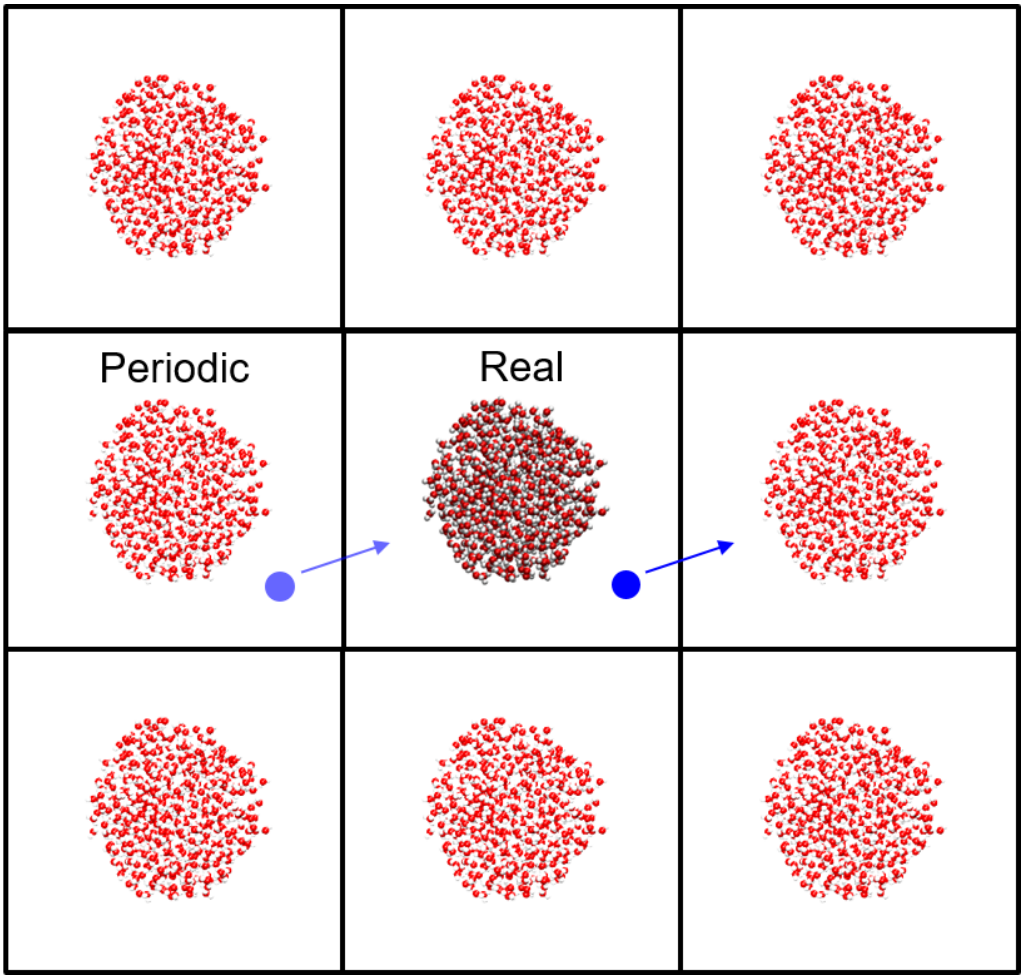

Figure 3.1: Illustration of periodic boundary conditions in MD simulation. This figure deals with 2-dimensional system with 1 real system and 8 periodic images. Blue dots and arrows represents the exit and reentrance of molecule in periodic system.

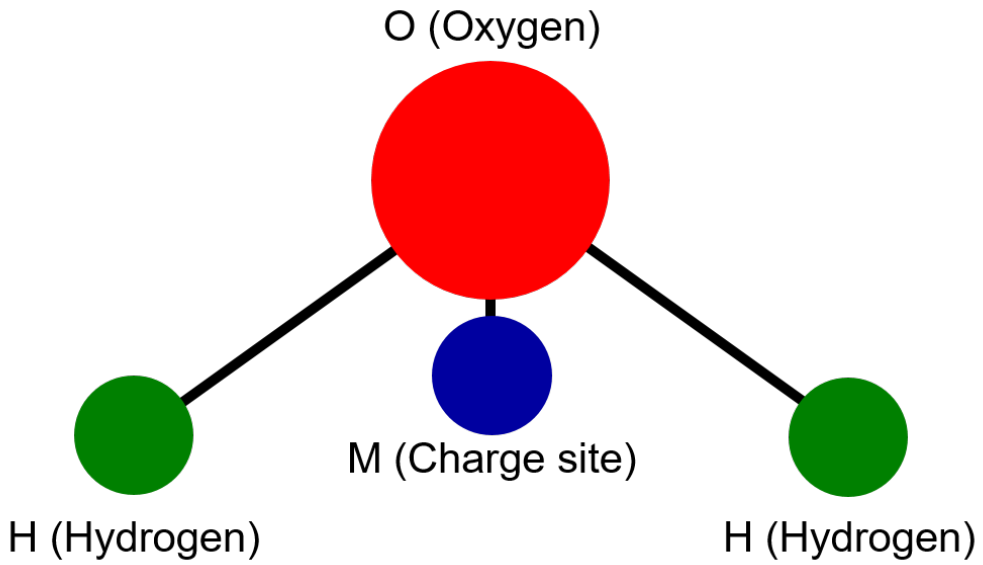

Figure 3.2: Illustration of TIP4P/2005 water model. Position of each atom is not same as real model for visual clarity.

Bibliography

[1] Allen, P. & Tildesley, D. J. *Computer Simulation of Liquids* (Oxford University, New York, 1987).

[2] Hockney, R. W., Goel, S. P. & Eastwood, J. *J. Comp. Phys.* **14**, 148-158 (1974).

[3] Abascal, J. L. F & Vega, C. A *J. Chem. Phys.* **123**, 234505 (2005).

[4] Lennard-Jones, J. E. *Proc. R. Soc. Lond. A* **106**, 463-477 (1924).

[5] Jorgensen, W. L., Maxwell, D. W. & Tirado-Rives, J. *J. Am. Chem. Soc.* **118**, 11225-11236 (1996).

[6] Maier, J. A. et al. *J. Chem. Theory Comput.* **11**, 3696-3713 (2015).

[7] Barker, J. A. & Watts, R. O. *Mol. Phys.* **26**, 789-792 (1973).

[8] Ewald, P. P. *Ann. Phys.* **64**, 253-287 (1921).

[9] Darden, T., York, D. & Pedersen, L. *J. Chem. Phys.* **98**, 10089-10092 (1993).

[10] Nose, S. *Mol. Phys.* **52**, 255-268 (1984).

[11] Hoover, W. G. *Phys. Rev. A.* **31**, 1695-1697 (1985).

[12] Berendsen, H. J. C., Postma, J. P. M., DiNola, A. & Haak, J. R. *J. Chem. Phys.* **81**, 3684-3690 (1984).

[13] Andersen, H. C. *J. Chem. Phys.* **72**, 2384 (1980).

[14] Basconi, J. E. & Shirts, M. R. *J. Chem. Theory Comput.* **9**, 2887-2899 (2013).

[15] Medders, G. R. & Paesani, F. *J. Chem. Theory Comput.* **11**, 1145-1154 (2015).

[16] Algara-Siller, G. et al. *Nature* **519**, 443-445 (2015).

[17] Russo, J. & Tanaka, H. *Nat. Comm.* **5**, 3556 (2014).

[18] Russo, J., Romano, F. & Tanaka, H. *Nat. Mat.* **13**, 733-739 (2014).

[19] Vega, C. & Abascal L. F. *J. Chem. Phys.* **125**, 034503 (2006).

[20] Jorgense, W. L. et al. *J. Chem. Phys.* **79**, 926-935 (1983).

[21] Berendsen, H. J. C., Grigera, J. R. & Straatsma, T. P. *J. Phys. Chem.* **91**, 6269-6271 (1987).

[22] Mahoney, M. W. & Jorgensen, W. L. *J. Chem. Phys.* **112**, 8910-8922 (2000).

[23] Lamoureux, G. et al. *Chem. Phys. Lett.* **418**, 241-245 (2005).

[24] Pronk, S. et al. *Bioinfomatics* **29**, 845-854 (2013)

[25] Plimpton, S. *J. Comp. Phys.* **117**, 1-19 (1995).

[26] Goetz, A. W. et al. *J. Chem. Theory Comput.* **8**, 1542-1555 (2012).

[27] Phillips, J. C. et al. *J. Comp. Cem.* **26**, 1781-1802 (2005).

[28] Todorov, I. T., Smith, W., Trachenko, K. & Dove, M. T. *J. Mater. Chem.* **16**, 1911-1918 (2006).

Chapter 4

Surface Tension of Water Nanodroplet using Molecular Dynamics Simulation

4.1 Introduction

In this chapter, we investigate the surface tension and Tolman length of TIP4P/2005 water nanodroplet with MD simulation. Surface tension of curved interface is described simply with Tolman's equation [1],

$$\frac{\gamma(R_{\mathrm{s}})}{\gamma_0} = 1 - \frac{2\delta_0}{R_{\mathrm{s}}} + O\left(\frac{1}{R_{\mathrm{s}}^2}\right), \tag{4.1}$$

where γ_0 is the surface tension of planar interface and δ_0 is the Tolman length $\delta(R_{\mathrm{s}})$ in limiting case at planar interface. Tolman length $\delta(R_{\mathrm{s}})$ is defined by the

difference between the equimolar radius R_e and surface of tension R_s as

$$\delta(R_s) = R_e - R_s. \tag{4.2}$$

Note that R_e is related with the shape of droplet and R_s is related with the interaction between molecules in droplet. Derivation of Eq. (4.1) is introduced in Chapter 2.

Even popularity and applicability of Tolman's equation, it has failed to explain experimental results in nanoscale [2]. Curvature expansion of the mean-field model of flat interface has shown that the surface tension of curved interface is explained with the polynomial series of curvature, including at least quadratic term [3–6]. These studies suggest that the Helfrich's equation with bending rigidity of the surface can describe surface tension of nanoscale [7].

$$\frac{\gamma_s(R_s)}{\gamma_0} = 1 - \frac{2\delta_0}{R_s} + \frac{k_s}{R_s^2} + O\left(\frac{1}{R_s^3}\right), \tag{4.3}$$

where k_s is the bending rigidity of the surface.

Even Helfrich's equation well describes the surface tension of curved interface, there are two issues which have been debated. The first issue considers the method of obtaining coefficient of quadratic term. While Tolman length has clear definition, bending rigidity in Helfrich's equation is rather phenomenological variable and have no molecular definition for obtaining it. Curvature expansion method shows limitation for study of real liquid molecules such as water because of its numerical complexity [8]. The second issue is about the debate between magnitude and the sign of Tolman length and bending rigidity.

Recent experiments with noble methods still give contradict results about the sign of Tolman length and bending rigidity [2, 9, 10].

In this chapter, we carry out the molecular dynamics of nanodroplet with TIP4P/2005 water model to resolve these issues. We obtain surface tension and Tolman length from radial pressure tensor and density profile of nanodroplet. Our results show that the Tolman length is a function of the radius of the nanodroplet and is not a constant. From Tolman length, we derive the quadratic equation of surface tension, which can be interpreted as the extended version of Tolman's equation. This equation predicts accurately the MD results of smallest nanodroplet we consider. Further analysis of the thermodynamics and dynamics of water molecules show that the variation of surface tension and Tolman length is due to the unexpected location of R_{s} in small nanodroplet, while R_{e} is at the expected location. Moved location of R_{s} is because interfacial water of small nanodroplet has lower hydrogen bonding and larger energy than large nanodroplet because they have smaller neighborhood to interact.

4.2 Preparation of system

We consider the liquid water nanodroplets consisting of between $N = 32$ ($R_{\mathrm{e}} \sim 0.6$ nm) and $N = 512$ ($R_{\mathrm{e}} \sim 1.5$ nm) TIP4P/2005 water molecules [11], where N is number of water molecules. The snapshots of two droplets are shown in Fig. 4.1. TIP4P/2005 water model is rigid water model without intramolecular vibration and thus O-H bonds length and the H-O-H angles of the water molecules

are constrained using the SHAKE algorithm [12] with a relative tolerance of 10^{-5}.

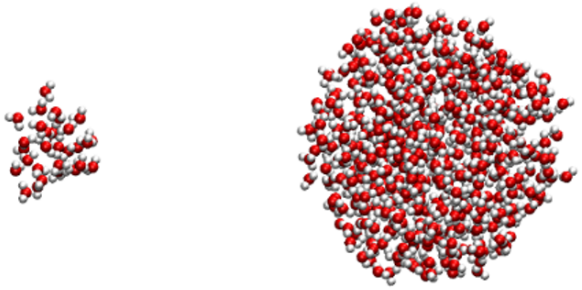

Figure 4.1: The snapshots of (left) $N = 32$, (right) $N = 512$ water nanodroplets. We omit the virtual charge in TIP4P/2005 water model and draw only oxygen and hydrogen atoms for visual clarity.

All simulations are carried out using the GROMACS 5.1.4 MD simulation package [13]. We perform simulations in the canonical ensemble, where the total number of molecules N, the volume of the system V, and the temperature of the whole system T are conserved. Temperature is controlled using a Nose-Hoover thermostat with a time constant of 1 ps. The prepared droplets are located in a center of simulation cell, with periodic boundary conditions in every directions. We choose length of simulation cell $L = 20$ nm and it is large enough to avoid any long-range interaction between the water droplet and its periodic images. We use cut-off scheme for calculating both Lennard-Jones and Coulomb interactions without any further correction algorithm for long-range interaction. The cut-off

length is set as half of length of simulation cell. The equations of motion are integrated using the leap-frog algorithm with a time step of 1 fs. The position and velocity of all molecules are collected each 0.1 ps during 100 ns simulation and thus we use 10^6 snapshots for analysis. The error bar is estimated as a standard deviation of results from 10 separate blocks of 10^5 snapshots.

4.3 Surface tension of water nanodroplet

4.3.1 Pressure tensor of spherical system

To calculate the distribution of normal $P_N(r)$ and tangential $P_T(r)$ components of the pressure tensor as a function of radial distance r from the center of mass of the water nanodroplet, we follow the perturbation method which is developed by Ghoufi *et al* [14] for a spherical symmetry. To obtain pressure distribution in local volume, we use the local partition function $\Xi(r)$ in the grand canonical ensemble, which can define a local grand potential $\Omega(r)$ and a local pressure of the spherical system $P(r)$ respectively:

$$\Omega(r) = -k_B T \ln \Xi(r), \tag{4.4}$$

$$P(r) = -\left(\frac{\partial \Omega(r)}{\partial V(r)}\right)_{\mu V(r) T}, \tag{4.5}$$

where μ is the chemical potential, $V(r)$ is the volume of the spherical shell with radius r. From the definition of grand potential, we obtain the following

expression for local pressure:

$$P(r) = \rho(r)k_BT - \left\langle \frac{\partial U(r)}{\partial V(r)} \right\rangle_{NVT}, \tag{4.6}$$

where $\rho(r)$ is the local density average. Equation 4.6 summarizes that the local pressure is calculated from a summation of local density energy and potential energy change from volume perturbation, which is called the free energy perturbation formalism (FEP) [15]. A reference state (0) is converted to a perturbed state (1) by compressing or expanding of spherical system according to transformation of center of mass: $\mathbf{r}_{\mathrm{CM}} \rightarrow (1+\xi)\mathbf{r}_{\mathrm{CM}}$. Thus, the expression of pressure given in Eq. 4.6 can be rewritten as

$$P(r) = \rho(r)k_BT - \lim_{\xi \to 0} \left\langle \frac{U^1(r) - U^0(r)}{V^1(r) - V^0(r)} \right\rangle_{NVT}, \tag{4.7}$$

where the rescaled volume is $V^1(r) = (1+\xi)^3 V^0(r)$.

The obtained profile $P(r)$ contains both normal and transverse components of pressure because the modification of water coordinate onto radial direction also involves the change of transverse distance between two molecules. To decompose $P(r)$ into $P_N(r)$ and $P_T(r)$, we use the mechanical equilibrium condition of spherical geometry [16],

$$P(r) = \frac{1}{3}P_N(r) + \frac{2}{3}P_T(r), \tag{4.8}$$

$$P_T(r) = P_N(r) + \frac{r}{2}\frac{\mathrm{d}P_N(r)}{\mathrm{d}r}. \tag{4.9}$$

Combining Eq. 4.8 and Eq. 4.9, we obtain the $P_N(r)$,

$$P_N(r) = \frac{1}{r^3}\int_0^r 3r'^2 P(r')\mathrm{d}r'. \tag{4.10}$$

$P_T(r)$ can be calculated with the Eq. 4.9.

To obtain the ∂U and ∂V, we exerts expansion ($\xi > 0$) and contraction ($\xi < 0$) to the coordiantes of MD snapshots and calculates corresponding $U^1(r)$ and $V^1(r)$ respectively. After the ensemble average is carried out over the configurations of the reference system 0. Here we use $\xi = 10^{-5}$.

The pressure profiles of $N = 512$ water nanodroplet is shown in Fig. 4.2. The pressure profile is well separated with the inside bulk-like liquid pressure and vapor pressure with interface. Bulk-like liquid pressure of this nanodroplet is roughly ~ 90 MPa which is composed of ideal gas term (black squares) and perturbation of configurational energy (purple circles). In transverse pressure profile (P_T, red triangles), there is a negative minimum at the interface and it indicates that the interface is under compression due to interaction between molecules at interface. There is no local minimum in normal pressure profile (P_N, blue triangles). Note that pronounced fluctuation of pressure profile is shown around the center of nanodroplet, which is due to the lack of sufficient amount of samples. To avoid the large statistical error from this fluctuation, we exclude pressure data in $r < 0.05$ nm when we analyze the pressure profile.

4.3.2 Surface tension

From the transverse and normal pressure tensor, we compute surface tension with Lovett's expressions [17]

$$\gamma = \int_0^\infty dr \left[P_N(r) - P_T(r) \right]. \tag{4.11}$$

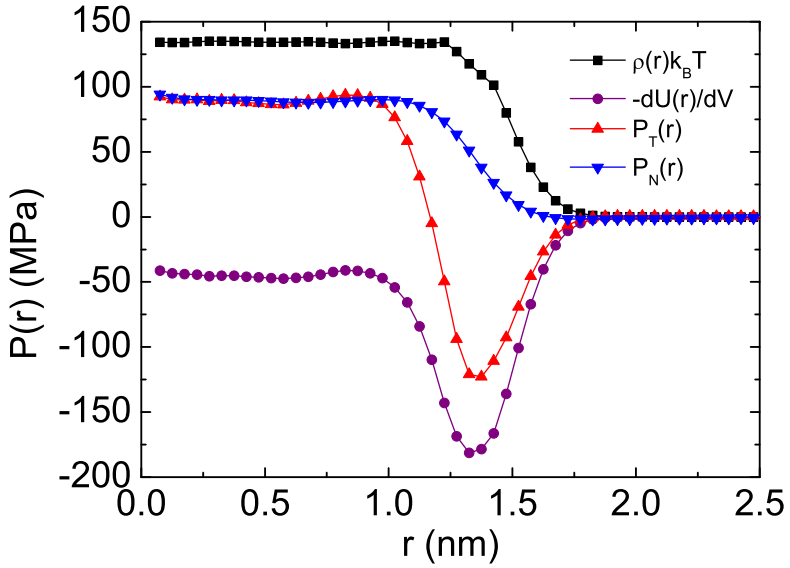

Figure 4.2: The pressure tensor of $N = 512$ nanodroplet.

Figure 4.3 shows normal pressure ($P_N(r)$), transverse pressure ($P_T(r)$) and their difference ($P_N(r) - P_T(r)$) of $N = 32, 128, 512$ nanodroplets. Pressures of center of nanodroplets follow the linear function of inverse radius, which is the Laplace relation $\Delta P = 2\gamma/R$. Note that amplitude of negative minimum of transverse pressure profile depends on the size of nanodroplet (Fig. 4.3 (b)). When $N = 32$, its amplitude is ~ -80 MPa while when $N = 512$, it reaches ~ -130 MPa. It indicates interaction between water molecules at interface in $N = 32$ droplet is weaker than large nanodroplet. Amplitude of negative minimum determines the maximum value of $P_N(r) - P_T(r)$, and it determines the surface tension of nanodroplet (Fig. 4.3 (c)). Figure 4.3 (d) shows that surface tension of nanodroplet is smaller than the tension of planar interface ($\gamma_0 = 65.9$ mN/m)

at $R_s < 0.8$ nm and is decreasing function of inverse radius. Note that when $R_s > 0.8$ nm, surface tension of nanodroplet does not remain at planar value and is $\gamma(R_s) > \gamma_0$. Because Tolman's equation (Eq. (4.1)) can describe only monotonic increase or decrease, this result evidences that Tolman's equation is not suitable for describing nanodroplet smaller than 1 nm.

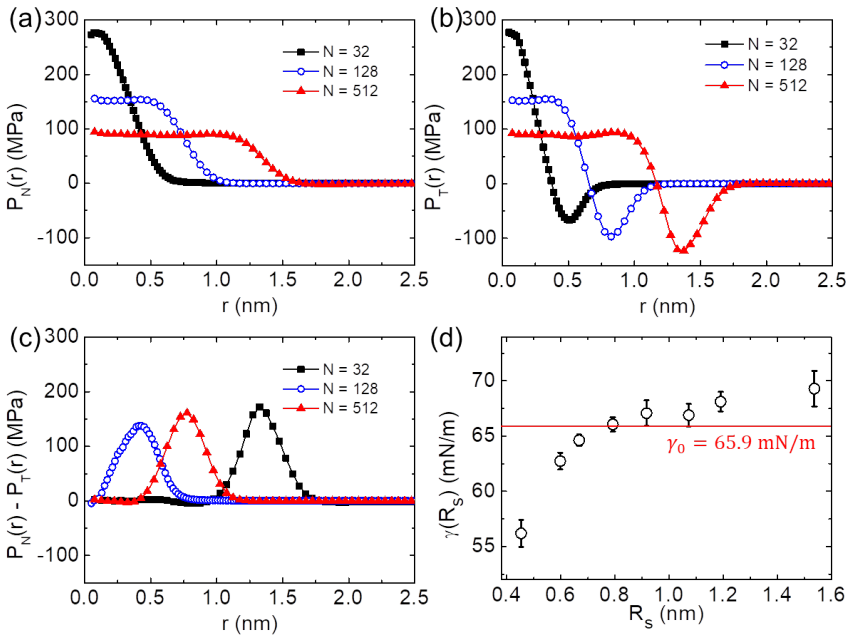

Figure 4.3: The (a) normal ($P_N(r)$), (b) transverse pressure ($P_T(r)$) and (c) $P_N(r) - P_T(r)$ of nanodroplet of $N = 32$, 128, and 512. (d) Surface tension of TIP4P/2005 water nanodroplet as a function of radius of surface R_s. Horizontal red line represents the surface tension of planar water-vapor interface $\gamma_0 = 65.9$ mN/m.

4.4 Equation of surface tension

In this section, we will derive the equation of surface tension which describes MD results accurately. Even Tolman's equation is popular and has been used widely, surface tension of TIP4P/2005 water nanodroplet we obtain (Fig. 4.3 (d)) indicates that it cannot be used when $R_s < 1$ nm, because surface tension is no more monotonic function in this scale. To derive a new equation, we follow the thermodynamic route introduced in Chapter 2 rather than fitting the MD results to the random equations. In chapter 2, relation between surface tension

and curvature is described by the differential equation so-called Gibbs-Tolman-Koenig-Buff (GTKB) equation. Tolman's equation can be obtained from GTKB equation with two assumptions, $\delta(R_\mathrm{s}) = \delta_0$ and $R_\mathrm{s} \gg \sigma$, where σ is molecular diameter. Exact solution of GTKB equation only can be achieved with the knowledge of correct form of Tolman length, $\delta(R_\mathrm{s})$ that Tolman's equation lacks. Here we compute Tolman length as a function of radius. It is possible in MD simulation because simulation gives information of configuration of every molecules in system. With Tolman length, we solve GTKB equation and obtain equation of surface tension, which is extended form of Tolman's equation. Derived equation can describe surface tension of $R_\mathrm{s} < 1$ nm and non-monotonic behavior of surface tension obtained from MD simulation.

4.4.1 Tolman length

Here, we calculate the Tolman length $\delta(R_\mathrm{s})$ of TIP4P/2005 water nanodroplet. Two definitions of radius, R_e and R_s, are defined as

$$\frac{4\pi {R_e}^3}{3}(\rho_\mathrm{l} - \rho_\mathrm{v}) = 4\pi \int_0^\infty \mathrm{d}r r^2 \left[\rho\left(r\right) - \rho_v\right], \tag{4.12}$$

$$P_\mathrm{l} - P_\mathrm{v} = \frac{2\gamma(R_\mathrm{s})}{R_\mathrm{s}}, \tag{4.13}$$

where ρ_l, ρ_v are the bulk density of liquid and vapor, P_l, P_v are the bulk pressure of liquid and vapor for corresponding thermodynamic condition, respectively. In definition of R_e, when temperature is far from critical temperature, ρ_v can be neglected and right side of equation equals N. In definition of R_s, note that

we do not use γ_0. If we use planar liquid-vapor surface tension, it is another definition of radius, so-called capillary radius.

Figure 4.4 shows Tolman length, $\delta(R_s)$, as a function of the inverse of surface of tension $1/R_s$. It shows that the Tolman length is not a constant and is the increasing function of $1/R_s$. To describe the Tolman length as a function of radius, we adopt the ansatz with the form, $\delta(R_s) = \delta_0 + \delta_1/R_s$ [2, 3, 18]. Note that when $R_s \to \infty$, $\delta(R_s) \to \delta_0$ and δ_0 can be understood as the Tolman length of planar interface. Line in Fig. 4.4 is the linear fitting curve and it well describes the MD results. We obtain $\delta_0 = -0.05877$ nm, $\delta_1 = 0.0927$ nm^2. Note that δ_0 and δ_1 have different units.

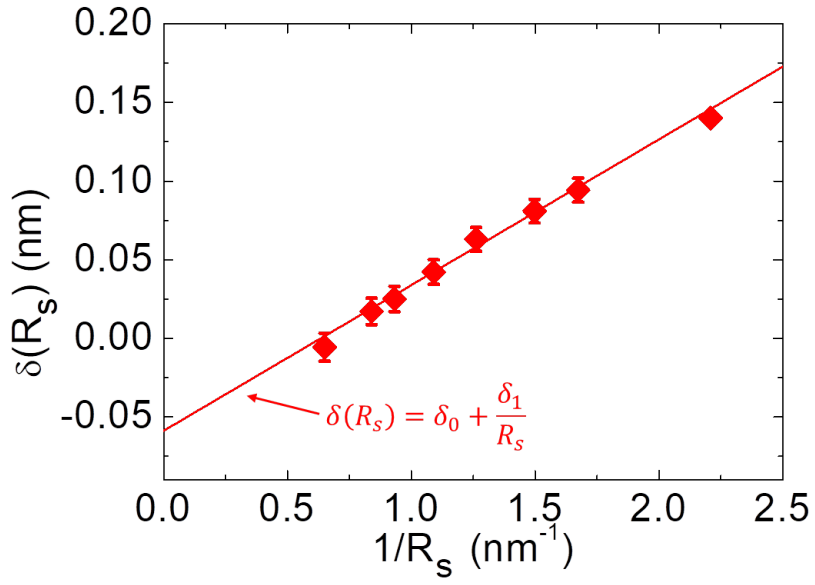

Figure 4.4: (dots) Tolman length, $\delta(R_s)$, of water nanodroplet as a function of inverse radius. (line) Fitting curve of Tolman length with $\delta(R_s) = \delta_0 + \delta_1/R_s$. The curve is drawn with δ_0 = -0.05877 nm, δ_1 = 0.0927 nm^2.

4.4.2 Derivation of equation of surface tension

From $\delta(R_\mathrm{s}) = \delta_0 + \delta_1/R_\mathrm{s}$ determined from previous section, we can derive the equation of surface tension by solving the Gibbs-Tolman-Koenig-Buff (GTKB) [19–22] equation given by

$$\frac{\mathrm{dln}\gamma}{\mathrm{dln}R_\mathrm{s}} = \frac{\frac{2\delta(R_\mathrm{s})}{R_\mathrm{s}}\left[1 + \frac{\delta(R_\mathrm{s})}{R_\mathrm{s}} + \frac{1}{3}\left(\frac{\delta(R_\mathrm{s})}{R_\mathrm{s}}\right)^2\right]}{1 + \frac{2\delta(R_\mathrm{s})}{R_\mathrm{s}}\left[1 + \frac{\delta(R_\mathrm{s})}{R_\mathrm{s}} + \frac{1}{3}\left(\frac{\delta(R_\mathrm{s})}{R_\mathrm{s}}\right)^2\right]} \tag{4.14}$$

via series expansion. The solution is truncated at the second order of curvature and it is explained as

$$\frac{\gamma(R_\mathrm{s})}{\gamma_0} = 1 - \frac{2\delta_0}{R_\mathrm{s}} + \frac{3\delta_0^2 - \delta_1}{R_\mathrm{s}^2} + O\left(\left(\frac{1}{R_\mathrm{s}}\right)^3\right). \tag{4.15}$$

When we consider only linear term of inverse radius, Eq. 4.15 reduces to Tolman's equation and it means that this equation can be considered as the extended version of Tolman's equation (Eq. 4.1) with the second order of curvature term for correction at smaller radius with new variable δ_1. To check the validity of Eq. 4.15, we draw the curve of the equation with the parameter δ_0 and δ_1 obtained from Fig. 4.4 and compare it with the surface tension from Fig. 4.3 (d). The comparison shows that the Eq. 4.15 predicts the surface tension of nanodroplet even the smallest size we deal with.

We quantitatively measure the accuracy of Eq. 4.15 and two other equations which have lower order, $\gamma(R_\mathrm{s})/\gamma_0 = 1$ and $\gamma(R_\mathrm{s})/\gamma_0 = 1 - 2\delta_0/R_\mathrm{s}$. Figure 4.6 shows that only considering second order term (Eq. 4.15) predict surface tension within ≤ 2 % error while other equations suffer from large error, ~ 50

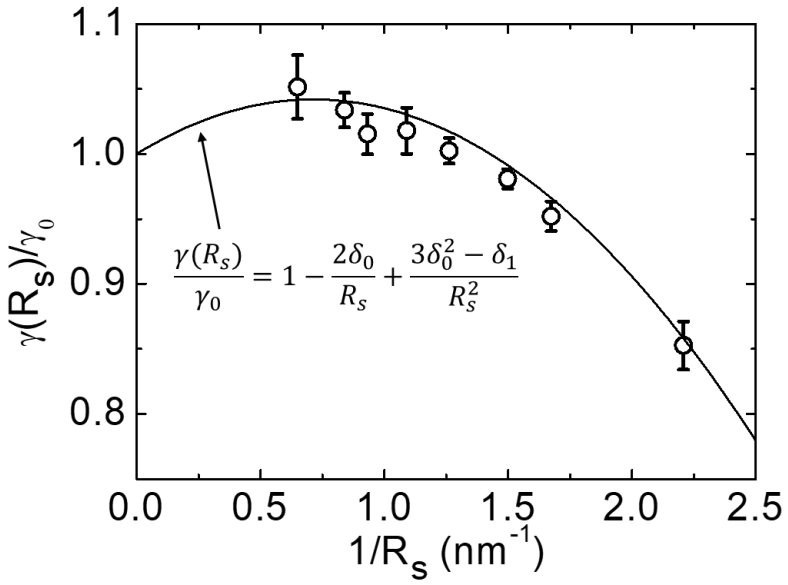

Figure 4.5: (dots) Surface tension of water nanodroplet normalized that of planar water-vapor interface as a function of inverse radius. (line) Equation of surface tension with δ_0 = -0.05877 nm, δ_1 = 0.0927 nm^2 obtained from Tolman length data.

%. Also the magnitude of error increases for decreasing droplet radius and it shows role of second order term for describing small nanodroplet. This result supports why we should use extended equation of Tolman's equation for dealing with nanodroplet.

4.4.3 Comparison with other results

Tolman length of the planar interface of water from MD is $\delta_0 = -0.59$Å, which is about one-sixth of molecule size and is consistent with the previous results. Wilhelmsen *et al.* used square gradient theory developed with equation of state

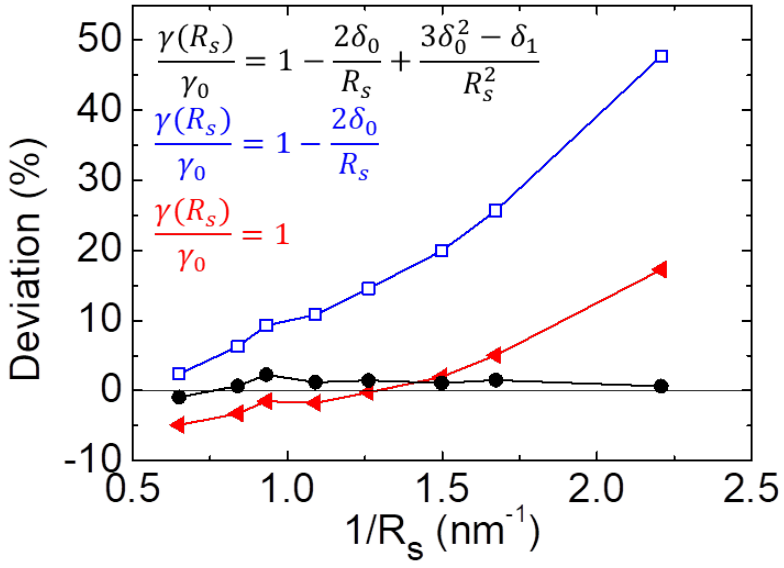

Figure 4.6: The error between surface tensions obtained from MD and prediction from three equations with different truncation order, $\gamma(R_s) = \gamma_0$, $\gamma(R_s) = \gamma_0 - 2\gamma_0\delta_0/R_s$, and $\gamma(R_s) = \gamma_0 - 2\gamma_0\delta_0/R_s + k_s/R_s^2$.

of water for combining with the cubic plus association equation and obtained $\delta_0 = -0.52$ Å [6]. Azouzi *et al.* estimated $\delta_0 = -0.47$ Å from measurements of rates of water cavitation in quartz inclusions [23]. Joswiak *et al.* used the mitosis method and calculated the required excess Helmholtz free energy to separate nanocluster to two subclusters of equal size and obtained $\delta_0 = -0.56$ Å [24].

Second order coefficient, $3\delta_0^2 - \delta_1$ of Eq. 4.15 also get physical meaning by comparing with Helfrich's equation (Eq. 4.3). In Helfrich's equation, coefficient of second order represents bending rigidity k_s of curved interface. Thus we obtain relation $k_s = \gamma_0(3\delta_0^2 - \delta_1)$. The bending rigidities of water nanodroplet $k_s = -1.34k_BT$. Sign and magnitude of this value is consistent with MD study of

Sedlmeier and Netz [25] about interface between hydrophobic solute and water, which gives $k_{\mathrm{s}} \approx -3k_BT$.

4.5 Origin of variation of Tolman length

In previous sections, we show that surface tension of water nanodroplet follows polynomial series of inverse radius and at least quadratic equation is required to describe surface tension properly. Also we show that the reason is that Tolman length is linear function of droplet inverse radius. Here we discuss about the origin of variation of Tolman length with the analysis including structure, thermodynamics, and dynamics of water molecules in nanodroplet. The results show that variation of Tolman length is due to the deviation of R_{s} relative to R_{e} because small nanodroplet has larger interacial free energy than large nanodroplet.

4.5.1 Comparison between R_{e} and R_{s}

In classical view, the heterogeneous system of two distinct phases are divided into the two bulk phases and thin interfacial profile considered as the excess properties [1]. If this structure changes in nanodroplet, we expect that the location of radius changes and thereby Tolman length $\delta(R_{\mathrm{s}})$ deviates from δ_0. Fig. 4.7 shows behavior of two radius as a function of the number of water molecules in MD simulation. The equimolar radius, R_{e}, well follows $N^{1/3}$ relation, which indicates spherical shape of nanodroplet is well preserved. However, the surface

of tension radius, R_s, is deviated from $N^{1/3}$ behavior in small scale and it implies that R_s, which is determined from the energetic structure of nanodroplet, is attributed to the change of Tolman length.

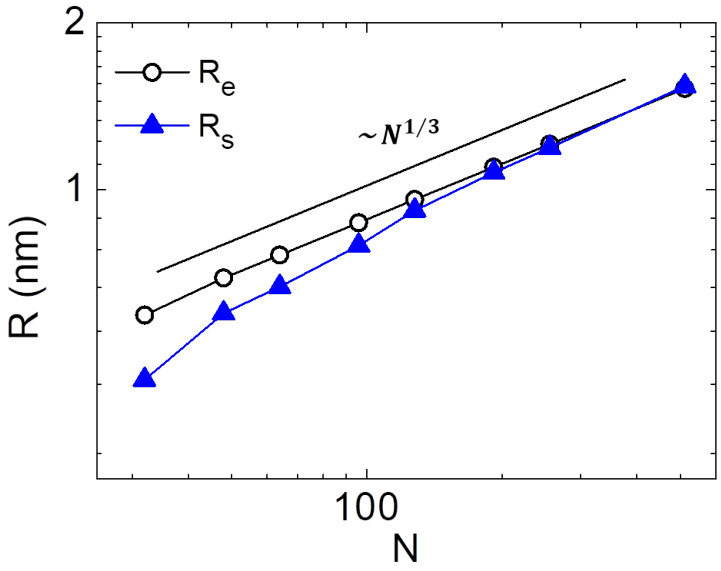

Figure 4.7: Comparison of R_e and R_s as a function of number of water molecule N. Black line is $\sim N^{1/3}$ and is drawn for guidance.

Fig. 4.8 shows how deviation of R_s occurs in small nanodroplet by comparing shape and energy profiles of $N = 32$ and $N = 512$ nanodroplets. Fig. 4.8 (a), (b) shows the radial density profiles of nanodroplet. In the $N = 512$ nanodroplet, density profile is decomposed into the bulk liquid, vapor and interface, and R_e locates on the mid-line of interface separating bulk liquid and vapor phase. Similar properties are shown in pressure, energy, hydrogen bond number profile (Fig. 4.8 (d), (f), (h)) and location of R_s is close to that of R_e. Also in $N = 32$ nanodroplet, the density profile preserves spherical shape

that of larger droplet. To check that the $n = 32$ retains spherical shape even its small radius, we obtain the 2D density profile of $n = 32$ nanodroplet (fig. 4.9). It clearly shows that nanodroplet can be considered spherical even 1D density profile shows pronounced oscillation along radial direction. From spherical 2D density profile, location of equimolar radius can be defined. Even density profile shows pronounced oscillaton, 2D mapping of density ensures that the nanodroplet is spherical. However, the energy-related profile of $N = 32$ droplet shows different shape with density profile (Fig. 4.8 (c)) and location of R_{s} moves inside of nanodroplet, which increases $\delta(R_{\mathrm{s}})$. When one sees the pressure, energy, hydrogen bond number profile of $N = 32$ nanodroplet (Fig. 4.8 (c), (e), (f)), the region with bulk-liquid pressure is small (r $<$ 0.2 nm). Even the water molecules at local maximum of density profile (r = 0.4 nm) lose $\sim$ 0.8 hydrogen bondings and gain $\sim$ 10 kJ/mol of energy relative center of droplet. Non-bulk structure in small nanodroplet also can be seen through mapping of orientiation distribution of water.

4.5.2 Thermodynamics of water nanodroplet

Here, we calculate energy, entropy, and Helmholtz free energy of water molecules in nanodroplet. Energy is easily obtained by calculate interaction between water molecules via Lennard-Jones and Coulomb interaction used in MD simulation. To calculate entropy, we use two-phase thermodynamics (2PT) model by integrating the density of states (DoS) function, which was first introduced from work of Lin *et al.* [26, 27]. 2PT model considers the liquid system as the sum of diffusive gaslike component and solidlike harmonic spring component. At first, DoS is determined from the Fourier transformation of the velocity autocorrelation function as

$$g(\nu) = \lim_{\tau\to\infty} \int_{-\tau}^{\tau} C(t)\exp(-i2\pi\nu t), \tag{4.16}$$

where $C(t)$ is autocorrelation function and is defined as

$$C(t) = \sum_j \lim_{\tau\to\infty} \frac{1}{2\tau} \int_{-\tau}^{\tau} \mathrm{d}t' v_j(t+t')v_j(t). \tag{4.17}$$

If the system is solid, harmonic oscillation dominates the mode of dynamics and diffusion can be neglected. However, the DoS of liquid has nonzero value of diffusional components DoS(0), which gives uncorrect entropy evaluation when one considers the system of liquid molecules only as the sum of harmonic oscillator. To avoid this, DoS is partitioned into a gaslike and solidlike components

$$g(\nu) = g^g(\nu) + g^s(\nu), \tag{4.18}$$

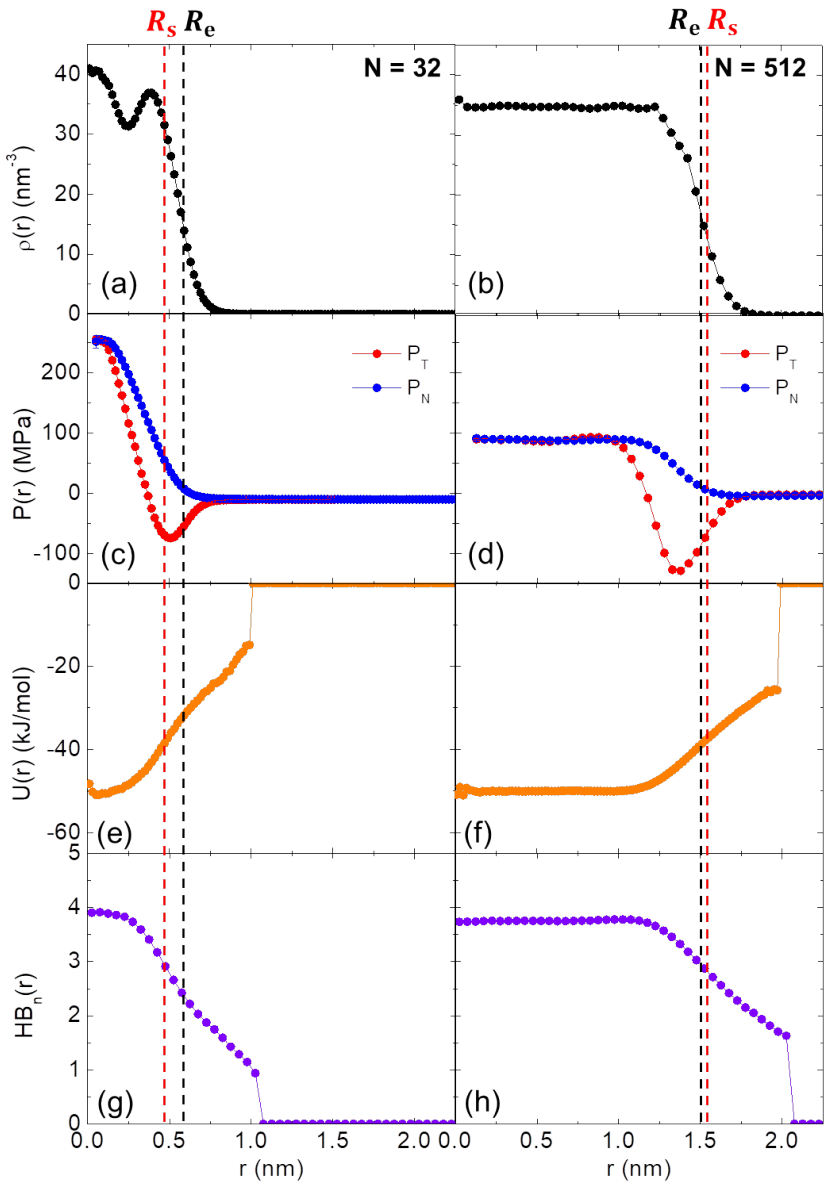

Figure 4.8: Radial profiles of two water nanodroplets of $N = 32$ (left column) and $N = 512$ (right column). (a), (b) Density profile. (c), (d) Pressure profile. (e), (f) Potential energy profile. (g), (h) Number of hydrogen bond profile. Blue and black horizontal lines are drawn for denoting the location of R_s and R_e respectively.

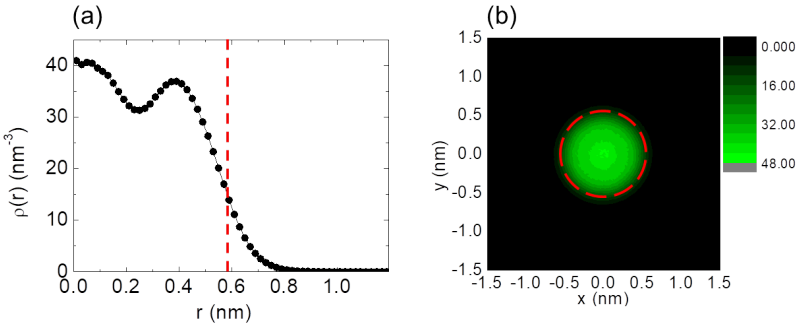

Figure 4.9: (a) 1D and (b) 2D density profiles of $n = 32$ nanodroplet. Red dotted lines denote location of equimolar radius R_{e}.

where $g^g(\nu)$ is the diffusive gaslike component and $g^{\mathrm{s}}(\nu)$ is solidlike component with harmonic motion. Here the $g^g(\nu)$ is expressed as

$$g^g(\nu) = \frac{g^g(0)}{1 + \left[\frac{\pi g^g(0)\nu}{6fN}\right]^2} \tag{4.19}$$

where f is the total degrees of freedom of the gas-like components and N is the number of molecules. For polyatomic molecules (e.g., water), each components also can be decomposed by the translation and rotation as

$$g^i(\nu) = g^i_{\mathrm{trn}}(\nu) + g^i_{\mathrm{rot}}(\nu), \tag{4.20}$$

where the $g^i_{\mathrm{trn}}(\nu)$ is determined from the center of mass velocities of molecules, $g^i_{\mathrm{rot}}(\nu)$ is determined from the angular velocity of molecules along the principal axis. Note that we do not consider vibrational velocity because TIP4P/2005 water model is rigid model.

Therefore, entropy S can be obtained from the sum of five contributions

$$S = S^g_{\mathrm{trn}} + S^g_{\mathrm{rot}} + S^{\mathrm{s}}_{\mathrm{trn}} + S^{\mathrm{s}}_{\mathrm{rot}}, \tag{4.21}$$

where each component is explained with the integration of DoS with weighting function

$$S_j^i = \int_0^\infty \mathrm{d}\nu g_j^i(\nu) W_j^i(\nu), \tag{4.22}$$

where $i = \{s, g\}$ and $j = \{\mathrm{trn}, \mathrm{rot}\}$.

Weighting function of solidlike component is written as the harmonic oscillator

$$W_j^{\mathrm{s}}(\nu) = \frac{\beta\hbar\nu}{\exp(\beta\hbar\nu) - 1} - \ln\left[1 - \exp(-\beta\hbar\nu)\right], \tag{4.23}$$

where $\beta = 1/k_B T$ and $\hbar = h/2\pi$, where h is the Planck's constant. The $W_{\mathrm{trn}}^g(\nu)$ is written as the

$$W_{\mathrm{trn}}^g(\nu) = \frac{1}{3}\frac{S^{\mathrm{HS}}}{k}, \tag{4.24}$$

where S^{HS} is the hard sphere entropy determined from the Carnahan-Starling equation of state. The $W_{\mathrm{rot}}^g(\nu)$ is written as the

$$W_{\mathrm{trn}}^g(\nu) = \frac{1}{3}\frac{S^{\mathrm{R}}}{k}, \tag{4.25}$$

where S^{R} is rotaitonal entropy of a rigid body.

Gaslike components of translational and rotational DoS are given by

$$g_{\mathrm{trn}}^g(\nu) = \frac{g_{\mathrm{trn}}^g(0)}{1 + \left[\frac{\pi g_{\mathrm{trn}}^g(0)\nu}{6fN}\right]^2} \tag{4.26}$$

$$g_{\mathrm{rot}}^g(\nu) = \frac{g_{\mathrm{rot}}^g(0)}{1 + \left[\frac{\pi g_{\mathrm{rot}}^g(0)\nu}{6fN}\right]^2} \tag{4.27}$$

If we obtain energy and entropy, Helholtz free energy F is easily calculated with relation $F = E - TS$, where T is temperature of system.

At first, we calculate the energy of every water molecule and plot its distribution as a histogram. Fig. 4.10 show histograms of energy distribution. We consider nanodroplet as the sum of two distinguised states, bulk and interface state, which incorporates the classical framework, and fit the histogram with two gaussian distribution curves. The results show that the average free energy of water molecules at interfacial state increases $\sim$ 3.9 kJ/mol in $N = 32$ nanodroplet. These evidence that the change of energy properties shown in Fig. 4.10 and deviation of R_{s} from relation $N^{1/3}$ are attributed to the change of interfacial energy.

Same analysis can be used to distribution of entropy and Helmholtz free energy(Fig. 4.11). Entropy also shows minor change whose magnitude $-TS \sim$ -2.2 kJ/mol. That is, total change of Helmholtz free energy, $\sim$ 6.1 kJ/mol between $N = 32$ and $N = 512$ water nanodroplet is mainly driven by potential energy of water molecules.

4.5.3 Dynamics of water nanodroplet

From thermodynamic analysis, the water molecule $N = 32$ nanodroplet has higher energy and one can expect it shows faster dynamics thatn that in $N = 512$ droplet. Here we use the VACF to observe the dynamics of water in nanodroplets. For detailed analysis we decompose the velocity of water into the translational and rotational velocity, and we calculate the VACFs of each (Fig. 4.12). The change of the VACF in different size of nanodroplet is clearly seen in both the translational and rotational VACF. For the translational VACF,

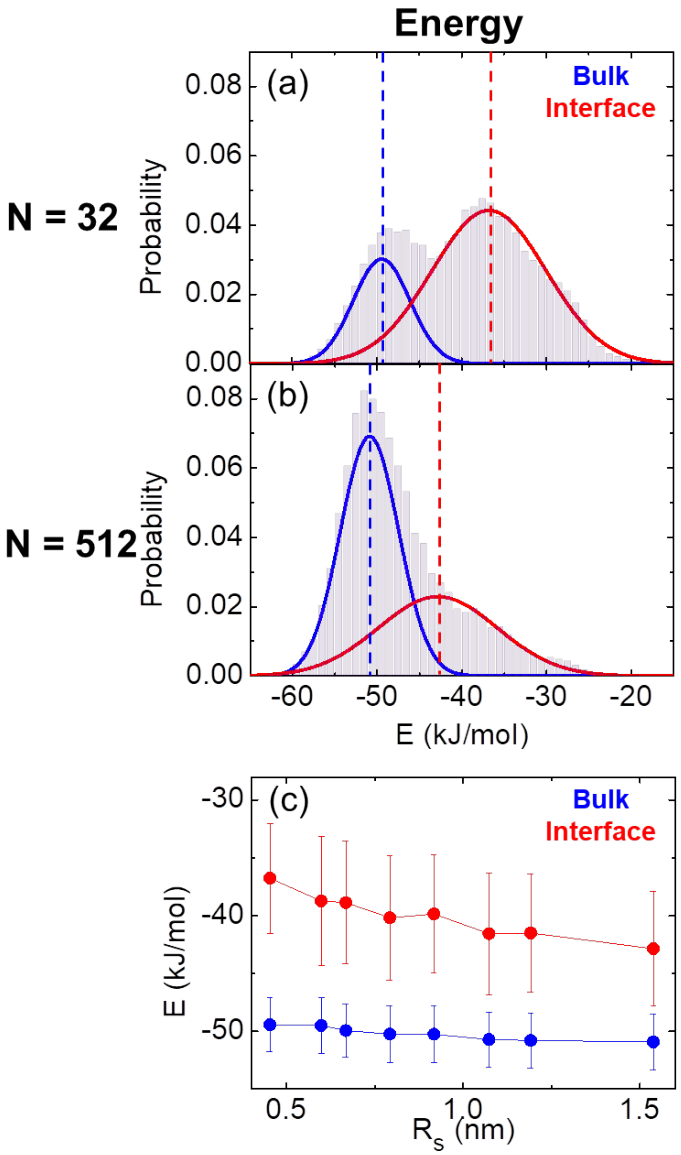

Figure 4.10: Distribution of energy of water molecules in (a) N = 32, (b) N = 512 nanodroplet. Bar denotes histogram drawn from MD results and solid lines denote fitting of results with double gaussian distributions, which indicate the water in bulk and interfacial state respectively. Dotted vertical lines denote location of the average of each gaussian distribution. (c) Average energy of bulk and interfacial molecules as a function of droplet radius.

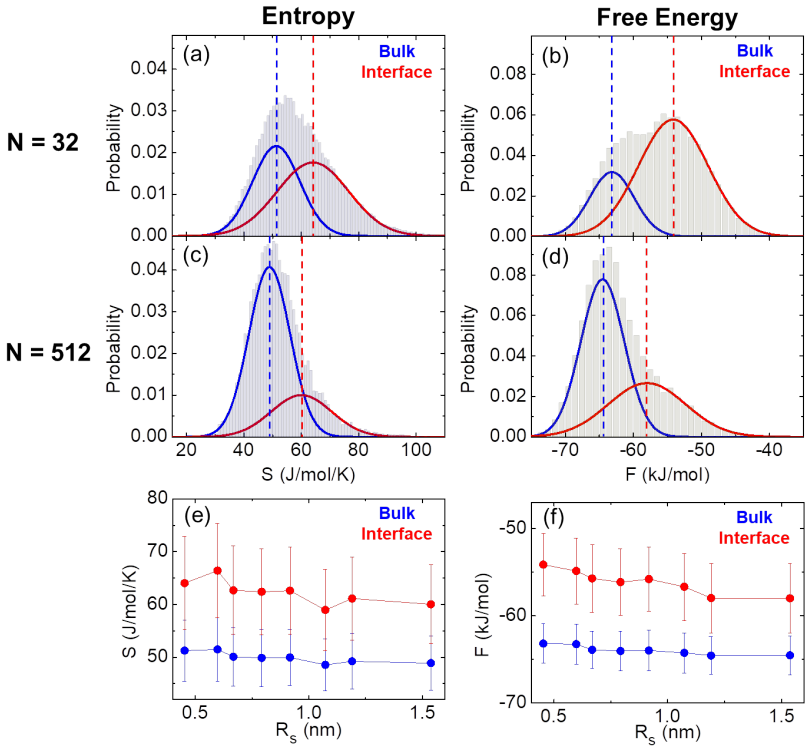

Figure 4.11: (a) - (d) Distribution of entropy and Helmholtz free energy of water molecules in N = 32, N = 512 nanodroplet. Bar denotes histogram drawn from MD results and solid lines denote fitting of results with double gaussian distributions, which indicate the water in bulk and interfacial state respectively. Dotted vertical lines denote location of the average of each gaussian distribution. Average (e) entropy and (f) Helmholtz free energy of bulk and interfacial molecules as a function of droplet radius.

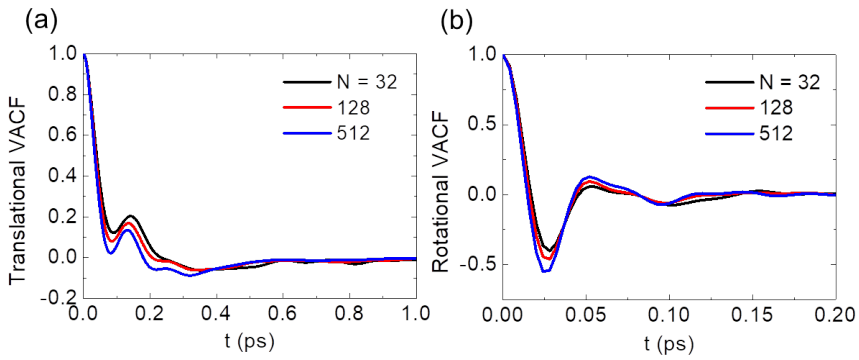

Figure 4.12: Averaged (a) translational and (b) rotational velocity autocorrelation functions of three different size of water nanodroplets with N = 32, 128, 512..

the negative minima around t = 0.1 ps disappears in $N = 32$ droplet. This disappearing minimum reveals the change of velocity due to collisions with the surrounding molecules decreases in $N = 32$ droplet. The rotational VACF also shows similar qualitative evidences of a rather free moving of water molecules in N = 32 droplet. The negative minima around t = 0.25 ps and well-defined oscillation at N = 512 droplet both decrease in N = 32 droplet.

The Fourier transforms of VACF gives the density of states (DOS), which gives information about the mode of dynamics. Figure 4.13 illustrates the translational and rotational power spectra in the frequency range of 0 - 400 cm^{-1} and 0 - 1200 cm^{-1} repectively and they also show strong dependence with nanodroplet size. In particular, the distinct upward shift of translational DOS in the low frequency with decreasing nanodroplet size indicates increased mobility of the water molecules due to decreasing number of first shell neighbors of the water molecule. The rotational DOS also shows a evidence of loosely bounded

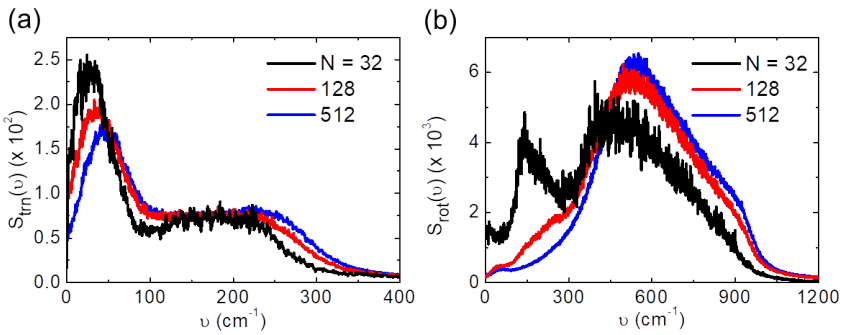

Figure 4.13: Averaged (a) translational and (b) rotational density of states of water molecules of three different size of water nanodroplets with N = 32, 128, 512..

molecule in small nanodroplet. The redshift of the libration peak around 600 cm^{-1} in small nanodroplet is observed. Note that the enhancement of the low-frequency modes of rotational motion of water inside the small nanodroplet, particularly in the 170 to 170 - 220 cm^{-1}, which represents the dynamics of vapor, evidences the high amount of broken bond. The pronounced peak around 200 cm^{-1} when $N = 32$ is similar to that of the water molecule confined in the (6, 6) hydrophobic carbon nanotube [28]. These results indicate that water molecule inside this nanodroplet is similar to the confined system and is different from the bulk liquid. These results gives evidence why energy profiles in small nanodroplet is different from that of large droplets and Tolman's assumption with constant Tolman length should be modified in the nanodroplet.

4.6 Conclusion

We report here a curvature dependence of surface tension of nanodroplet from the investigation of Tolman length from the molecular dynamics simulation with TIP4P/2005 molecular water model. Tolman length in nanoscale is function of radius and the polynomial equation of curvature up to second order can be obtained by solving GTKB equation with series expansion. Because water molecules inside small nanodroplet show unique properties, which is like in the confined system, thermodynamic properties of nanodroplet changes and gap between equimolar radius and radius of surface tension increases, which makes Tolman length as the function of radius. These results not only explain the properties of nanodroplet, also imply that this nanoscale system as a new solvent platform for driving unique interaction between solutes, which is not seen in bulk solvent.

Bibliography

[1] Tolman, R. C. *J. Chem. Phys.* **17** 333 (1949).

[2] Bruot, N. & Caupin, F. *Phys. Rev. Lett.* **116**, 056102 (2016).

[3] Block, B. J., Das, S. K., Oettel, M., Virnau, P. & Binder, K. *J. Chem. Phys.* **133**, 154702 (2010).

[4] Blokhuis, E. M. & van Giessen, A. E. *J. Phys.: Condens. Matter* **25**, 225003 (2013).

[5] Blokhuis, E. M. *J. Chem. Phys.* **138**, 194711 (2013).

[6] Wilhelmsen, O., Bedeaux, D. & Reguera, D. *J. Chem. Phys.* **142**, 171103 (2015).

[7] Helfrich, W. *Z. Naturforsch. C* **28**, (1973).

[8] Blokhuis, E. M. *Phys. Rev. E* **87**, 022401 (2013).

[9] Nguyen, V. D., Schoemaker, F. C., Blokhuis, E. M. & Schall, P. *Phys. Rev. Lett.* **121**, 246102 (2018).

[10] Kim, S., Kim, D., Kim. J., An. S & Jhe. W. *Phys. Rev. X* **8**, 041046 (2018).

[11] Abascal, J. L. F & Vega, C. *J. Chem. Phys.* **123**, 234505 (2005).

[12] Ryckaert, J. P., Ciccotti, G. & Berendsen, H. J. C. *J. Comput. Phys.* **23**, 327-341 (1977).

[13] Pronk, S. et al. *Bioinfomatics* **29**, 845-854 (2013).z

[14] Ghoufi, A. & Malfreyt, P. *J. Chem. Phys.* **135**, 104105 (2011).

[15] Gloor, G. J., Jackson, G., Blas, F. J. & de Miguel, E. *J. Chem. Phys.* **123**, 134703 (2005).

[16] Thompson, S. M. et al *J. Chem. Phys.* **81**, 530 (1984).

[17] Lovett, R. & Baus, M. *J. Chem. Phys.* **106**, 635 (1997).

[18] Baidakov, V. G. & Bobrov, K. S. *J. Chem. Phys.* **140**, 184506 (2014).

[19] Gibbs, J. W., Bumstead, H. A. & van Name, R. G. *Scientific Papers of J. Willard Gibbs: Thermodynamics* (Longmans and Green, New York).

[20] Koenig, F. O. *J. Chem. Phys.* **18**, 449 (1950).

[21] Buff, F. P. *J. Chem. Phys.* **19**, 1591 (1951).

[22] Rowlinson, J. C. & Widom, B. *Molecular Theory of Capillarity* (Clarendon, Oxford, 1982).

[23] Azouzi, M. E. M., Ramboz, C., Lenain, J. F. & Caupin, F. *Nat. Phys.* **9**, 38-41 (2013).

[24] Joswiak, M. N., Duff, N., Doherty, M. F. & Peters, B. *J. Phys. Chem. Lett.* **4**, 4267-4272 (2013).

[25] Sedlmeier, F. & Netz, R. R. *J. Chem. Phys.* **137**, 135102 (2012).

[26] Lin, S. T., Blanco, M. & Goddar, W. A. *J. Chem. Phys.* **119**, 11792 (2003).

[27] Huang, S. N., Pascal, T. A., Goddard, W. A., Maiti, P. K. & Lin, S. T. *J. Chem. Theory Comput.* **115**, 14190-14195 (2011).

[28] Pascal, T. A., Goddard, W. A. & Jung, Y. *Proc. Natl. Acad. Sci. USA* **108**, 11794-11798 (2011).

Chapter 5

Surface Tension of Liquid Nanodroplet using Density Functional Theory

5.1 Introduction

In previous chapter, we investigate the surface tension of water nanodroplet using MD simulation. From analysis of Tolman length, we derive the equation of surface tension which predicts the MD results. Here we use density functional theory (DFT) for investigating nanodroplet system and confirm that the approached used in MD simulation and water nanodroplet is applicable in other methods and other liquids.

5.2 Density functional theory of liquid

In DFT, thermodynamic quantities of liquid system are considred as the integration of density functional. In the open system, the grand potential $\Omega[\rho(\mathbf{r})]$ corresponding to the inhomogeneous density profile $\rho(\mathbf{r})$ is defined as [1]

$$\Omega[\rho(\mathbf{r})] = F[\rho(\mathbf{r})] - \mu \int \mathrm{d}\mathbf{r}\rho(\mathbf{r}), \tag{5.1}$$

where F is the Helmholtz free energy and μ is the chemical potential of the system. The Helmholtz free energy is divided into the hard sphere energy of repulsion and the attractive energy:

$$F[\rho(\mathbf{r})] = F_{\mathrm{hs}}[\rho(\mathbf{r})] + \frac{1}{2}\int \mathrm{d}\mathbf{r}\int \mathrm{d}\mathbf{r}'\rho(\mathbf{r})\rho(\mathbf{r}')U_{\mathrm{att}}(|\mathbf{r}-\mathbf{r}'|) \tag{5.2}$$

In Eq. (5.2), attractive energy is considered as a mean-field average of density functionals and further correlations are omitted. The attractive potential is based on the truncated Lennard-Jones potential according to Weeks-Chandler-Andersen perturbation theory [2]:

$$U_{\mathrm{att}}(r) = \begin{cases} -\epsilon & r \le r_{\min}, \\ 4\epsilon\left[\left(\frac{\sigma}{r}\right)^{12} - \left(\frac{\sigma}{r}\right)^{6}\right] & r_{\min} < r < r_{\mathrm{c}}, \\ 0 & r > r_{\mathrm{c}} \end{cases} \tag{5.3}$$

where σ is the diameter of liquid molecule. To calculate the free energy of a hard sphere part we consider the Carnahan-Starling form [3]:

$$F_{\mathrm{hs}}(\rho) = k_{\mathrm{B}}T\rho\ln(\rho) + k_{\mathrm{B}}T\rho\frac{(4\eta - 3\eta^2)}{(1-\eta)^2} \tag{5.4}$$

where η is defined as the $\eta = (\pi/6)\,\rho\sigma^3$.

The goal of DFT is finding density functional of the equilibrium system on the minimum of the grand potential. If there is no other local minima, it can be obtained by finding solution of $\delta\Omega/\delta\rho(r) = 0$. This is explained by functional derivative of Eq. (5.1) as

$$\mu = \frac{\delta F_{\mathrm{hs}}\left[\rho\left(\mathbf{r}\right)\right]}{\delta\rho\left(\mathbf{r}\right)} + \int \mathrm{d}\mathbf{r}'\rho\left(\mathbf{r}'\right) U_{\mathrm{att}}\left(\left|\mathbf{r}-\mathbf{r}'\right|\right) \tag{5.5}$$

5.3 Preparation of the system

DFT use reduced units: $r^* = r/\sigma$, $R^* = R/\sigma$, $\delta^* = \delta/\sigma$, $\rho^* = \rho\sigma^3$, $T^* = T/T_c$, where σ is the diameter of the liquid molecule and T_c is the critical temperature of liquid. Here we choose $T^* = 0.53 - 0.91$, which embraces the broad range of temperature. For comparison, we bring the TIP4P/2005 MD result from previous chapter and we use $T_c = 641.4$ K and $\sigma = 0.3159$ nm to use reduced unit [4]. We choose the range of nanodroplet radius as $R^* = 1.77 - 30$. When $R^* = 30$, the real size of nanodroplet exceeds 10 nm, which requires heavy computer resources if one uses MD simulation. It is possible in DFT because symmetry of system can reduce 3-dimensional system into 1-dimensional system along radial direction. All DFT calculations are carried out home-made code implemented by C language.

For calculation of density profile of critical spherical nanodroplet, we need to know that the system is located at the saddle point of the potential curve, not its minimum energy. The simple minimization methods used in DFT yield

only two types of divergences in this case: $R_s = 0$ or $R_s = \infty$. The path of divergence is determined from the initial radius of the droplet R_i. If the initial radius $R_{i,1}$ of the droplet is less than the critical radius R_c, then $R_{i,1} \to 0$ and in the opposite case the initial radius $R_{i,2}$ becomes $R_{i,2} \to \infty$. That is, we need to find R_c and use it as the initial radius. To find R_c, we iterate up to find two initial radii which satisfy $R_{i,1,\max} - R_{i,2,\min} < \sigma/100$ and from these we define the critical radius as the $R_c = (R_{i,1,\max} - R_{i,2,\min})/2$. To find the density profile of the critical droplet, we monitor the change of Ω for the iteration step n and we find n^* which satisfies $\frac{\mathrm{d}^2\Omega}{\mathrm{d}n^2}|_{n=n^*} = 0$ and obtain the density profile $\rho(r)$ of the critical droplet [5].

5.4 Tolman length and surface tension of liquid nanodroplets

At first, we obtain the surface tension from density functional. Because DFT uses thermodynamic potentials directly, surface tension can be obtained from density profile. From the grand potential Ω and radial density profile $\rho(r)$, one can define surface tension $\gamma(R_s)$ from the excess energy required to nucleate the droplet from pure vapor $\Delta\Omega$:

$$\frac{\Delta\Omega}{A} = -\frac{\Delta p}{3} R_s + \gamma\left(R_s\right) \tag{5.6}$$

where $\Delta\Omega = \Omega + p_v V$, $\Delta p = p_l - p_v$ and p_l and p_v are the bulk pressure of liquid and vapor phase respectively.

For study about Tolman length, we need to define the surface of tension R_s and equimolar radius R_e. Surface of tension is defined from relation $\frac{\mathrm{d}\gamma}{\mathrm{d}R}|_{R_s} = 0$ [6] and obtained via differentiating equation (5.6) as

$$R_s{}^3 = \left(\frac{3\Delta\Omega}{2\pi\Delta p}\right) \tag{5.7}$$

and we can obtain equimolar radius R_e as [7]

$$R_e{}^3 = \frac{3}{\Delta\rho}\int_0^\infty \mathrm{d}r r^2 \left[\rho\left(r\right) - \rho_v\right] \tag{5.8}$$

where $\Delta\rho = \rho_l - \rho_v$ and ρ_l and ρ_v are the bulk density of liquid and vapor phase respectively.

Figure 5.1 shows Tolman length, $\delta^*(R_s^*) = R_e^* - R_s^*$, as a function of the inverse radius $1/R_s^*$. It shows that the Tolman length from DFT also follows linear relation with inverse radius, which is same as we observed in MD simulation of water nanodroplet. Lines in Fig. 5.1 indicate the linear fitting curve and the corresponding value of δ_0^*, δ_1^* and k_s^* defined with relation $k_\mathrm{s}^* = \gamma_0^*(3\delta_0^{*2} - \delta_1^*)$ are summarized in Table 5.1.

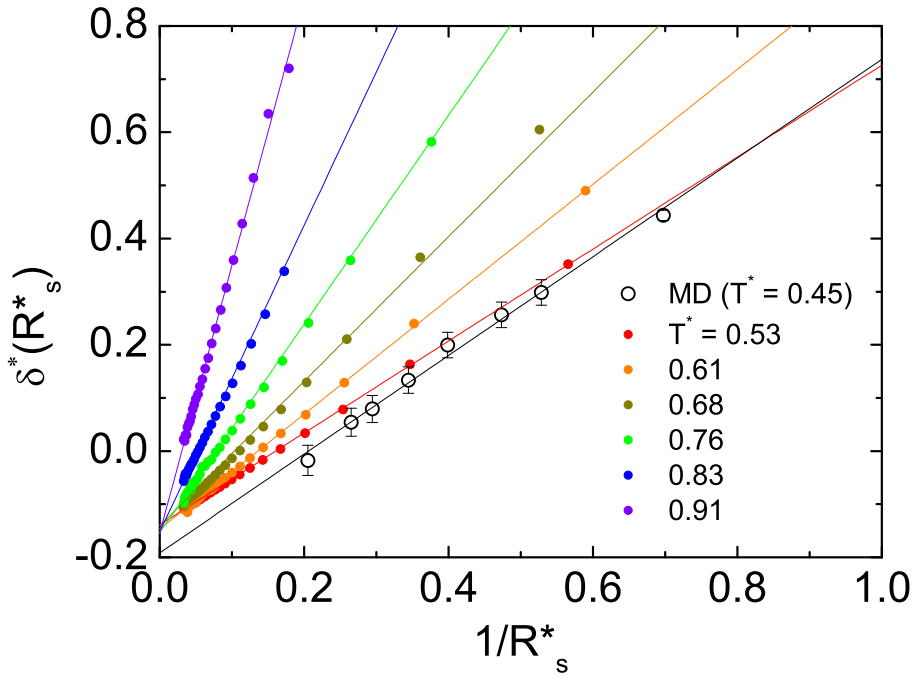

Figure 5.1: The MD and DFT results of Tolman length $\delta^*(R_s^*)$ as a function of inverse radius of the nanodroplet $1/R_s^*$. Lines indicate fitting of the MD and DFT results (dots) with the equation $\delta^*(R_s^*) = \delta_0^* + \delta_1^*/R_s^*$.

The Table 5.1 show that nanoscale surface tension of droplet can be considered with general equation with negative δ_0 and positive δ_1. The signs of them are same at every temperature we consider. From parameters in Table 5.1, we compare surface tension and equation of surface tension derived in Chapter 4,

$$\frac{\gamma(R_\mathrm{s})}{\gamma_0} = 1 - \frac{2\delta_0}{R_\mathrm{s}} + \frac{3\delta_0^2 - \delta_1}{R_\mathrm{s}^2} + O\left(\left(\frac{1}{R_\mathrm{s}}\right)^3\right) \tag{5.9}$$

which is shown in Fig. 5.2. As expected from Tolman length, Eq. (5.9) predicts surface tension of DFT with good accuracy. We can observe some trends of

Table 5.1: Tolman length and bending rigidity of nanodroplets of MD and DFT results

T^* (DFT)	δ_0^*	δ_1^*	k_s^*
0.53	-0.139	0.865	-0.807
0.61	-0.147	1.082	-0.717
0.68	-0.141	1.261	-0.501
0.76	-0.165	1.965	-0.382
0.83	-0.164	2.886	-0.285
0.91	-0.155	5.040	-0.197
T (MD)	δ_0	δ_1	k_s
290 K	-0.59 (Å)	9.27 (Å^2)	-1.34 ($k_{\mathrm{B}}T$)

surface tension in different temperature. In lowest temperature we consider(MD at $T^* = 0.45$), surface tension is smaller than planar surface tension when $1/R_s^* \sim 0.4$. If temperature increases, this cutoff radius also increases and when $T^* = 0.83$, it is $1/R_s^* \sim 1.5$. It indicates that the nanodroplet surface tension changes easily from planar interface when temperature increases and approaches close to critical temperature.

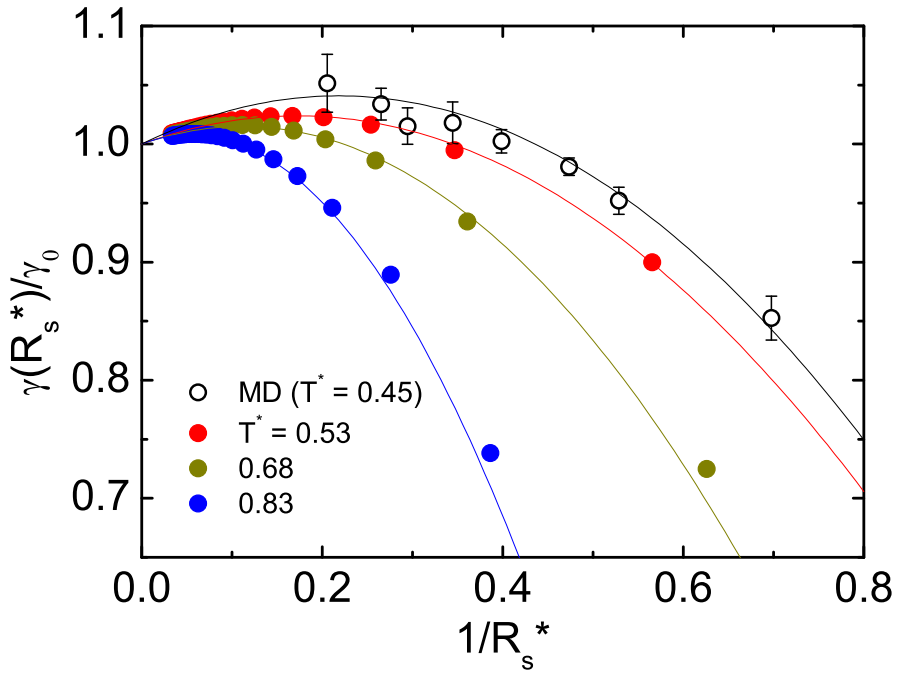

Figure 5.2: The comparison of surface tension obtained from the MD, DFT (dots) and theoretical prediction (lines). δ_0^* and δ_1^* are obtained from the Tolman length data in Fig. 5.1.

5.5 Conclusion

Here we obtain surface tension and Tolman length of nanoscale liquid droplet using DFT. With DFT we consider simple liquid molecule with Lennard-Jones interaction at broad range of temperature, which is close to critical temperature. Even we use different kind of liquid molecules, DFT gives same result as MD in both Tolman length and surface tension. This indicates that the discussion we have about MD simulation of water nanodroplet can be applied to DFT without further correction. It implies that our surface tension study based on Tolman

length and thermodynamic GTKB equation can be applied to broad range of temperature and various kinds of liquid.

Bibliography

[1] Hanse, J. P. & McDonald, I. R. *Theory of simple liquids* (Academic, London, 2006).

[2] Weeks, J. D., Chandler, D. & Anderson, H. C. *J. Chem. Phys.* **54**, 5237 (1971).

[3] Carnahan, N. F. & Starling, K. E. *Phys. Rev. A* **1**, 1672 (1970).

[4] Vega, C., Abascal, J. L. F. & Nezbeda, I. *J. Chem. Phys.* **124**, 074507 (2006).

[5] Zeng, X. C. & Oxtoby, D. W. *J. Chem. Phys.* **94**, 4472 (1991).

[6] Rowlinson, J. S. & Widom, B. *Molecular theory of capillarity* (Clarendon, Oxford, 1982).

[7] Gibbs, J. W. *Collected works* (Dover, New York, 1961).

Chapter 6

Conclusion

Interface between different phases is ubiquitous in nature and surface tension is one of important physical quantities which controls properties of interface and related phenomenas. Application of surface tension ranges from nucleation of nanoscale droplet and bubble in homogeneous phase to control of accumulation rate or interaction rate of molecules on surface. Despite of its importance, the precise description of surface tension of curved interface in nanoscale still remains unsolved problem. There are still debates about surface tension difference between nanodroplet and planar interface. Even there are broad range of studies such as Monte Carlo simulation, MD simulation, DFT, nucleation experiment, colloidal experiment, and atomic force microscopy experiment, there are still discrepancies between them. Because nanoscale droplet is composed of few tens or hundreds of molecules, the molecules are expected to show different properties with properties in planar interface, which can be the origin of

change of surface tension in nanoscale. MD simulation gives time trajectories of each molecule in system and one can analyze properties of molecules in single molecule resolution, which makes molecule dynamics simulations as the best fits for studying surface tension in nanoscale.

We carry out MD simulation of nanodroplet of TIP4P/2005 model water molecules from 32 molecules cluster to 512 molecules cluster. Their size ranges from $\sim$ 0.6 nm to $\sim$ 1.5 nm. Because MD gives time series of position of every molecules, we compute radial pressure tensors from potential energy perturbation and obtain surface tension. The results show that the surface tension of nanodroplet smaller than $\sim$ 0.8 nm has a smaller tension than that of planar interface. The shape of pressure tensor shows that it is because change of interaction between water molecules on interface.

We also derive the general equation of surface tension of nanoscale droplet. We study the Tolman length of nanodroplet from MD and solve GTKB equation with computed Tolman length. The solution is expanded as a polynomial series of inverse radius and resulting equation is quadratic, which is interpreted as the extension of Tolman's equation. The derived equation shows remarkable accuracy for predicting the surface tension of nanodroplet with < 2 % of error. Further analysis about structure, thermodynamics, dynamics of water molecules reveal that the increasing free energy of interfacial molecule accompanying with decreasing number of neighbor and faster dynamics changes surface tension at nanoscale.

To check whether the results we obtain is limited for water and MD

simulation method, we adopt DFT method to calculate the surface tension and Tolman length of liquid nanodroplet. In this study, we use Lennard-Jones simple liquid which is different with water. The DFT results show that same formalism used in water nanodroplet can be used in simple liquid results from DFT. It indicates that the method and formalism in this thesis can generally describe surface tension of liquid nanodroplet.

Our study provides prominent results to understand the surface tension of water nanodroplet. It can contribute to reduce discrepancy between many studies by providing general formalism. Also study shows that water molecules in nanodrolet have different properties and can act as a new kind of water-vapor platform.

초 록

표면 장력은 대기 중의 액체 방울의 응축 혹은 증발과 같은 상전이 현상을 결정짓는다. 그중에서도 1 나노미터 크기의 결정 핵에 대한 이해는 이 영역 대에서 생성되는 응축 에너지 장벽이 안정적인 액체 방울의 성장을 보장하기 때문에 특별히 중요성을 가진다. 그동안 나노물방울의 응축 실험 및 몬테 카를로 시뮬레이션, 분자 동역학 시뮬레이션, 밀도 범함수 이론 등의 방법을 통해 많은 관련 연구가 수행되었지만, 결과들을 종합해 보았을 때 여전히 나노물방울의 표면장력이 평평한 표면의 장력보다 큰지, 작은지, 혹은 변화가 없는지에 대한 명확한 이해가 불충분하다. 나노물방울이 수십 혹은 수백 개의 물분자로 이루어져 있다는 사실을 고려할 때 정확한 연구를 위해서는 단일 분자 수준의 정보를 줄 수 있는 방법을 이용하여야 한다.

본 연구에서는 (1) 분자 동역학 시뮬레이션과 그로부터 유도한 압력 텐서를 이용하여 최소 0.6 nm의 크기를 가진 작은 나노물방울의 표면 장력을 구하였다. 분자 동역학은 시스템 내부의 개개의 분자의 상호작용을 고려하기 때문에 이러한 작은 시스템을 다루는 데 적합하다. 결과로부터 나노물방울의 크기가 1 nm 보다 작을 경우 표면 장력의 크기가 작아지기 시작해서 평평한 표면의 표면장력의 80 퍼센트까지 감소하는 것을 확인하였다. (2) 분자 동역학 결과로부터 톨만 길이의 관계식을 구하고 이를 이용하여 나노물방울의 표면장력의 변화를 정확히 설명하는 표면 장력 식을 유도하였다. 이는 기존의 표면장력에 관한 식, 특히 톨만의 방정식이 왜 1 nm 미만 크기의 물방울을 설명하지 못하는지를 설명해준다. 또한 분자 동역학 시뮬레이션 뿐만 아니라 밀도함수 이론을 이용하여 이러한 주장이

넓은 범위의 온도에 대해서 유효함을 보였다. 물 분자의 열역학적 성질에 관한 추가적 분석은 이러한 표면장력의 특징이 물방울 표면에 분포하는 표면 물 분자들의 자유에너지의 증가 때문이라는 사실을 보여준다.

나노물방울의 표면 장력에 관한 연구는 나노물방울 표면의 수소결합 네트워크가 느슨해지는 것 때문에 표면 장력이 감소한다는 것을 보여준다. 액체-기체 표면에서 일어나는 분자의 흡착이 표면의 수소결합을 교란시키며 일어난다는 사실을 고려해 볼 때, 이러한 결과는 나노물방울과 다른 분자간의 상호작용에 관한 연구가 기존의 거시적인 표면에서 볼 수 없었던 새로운 결과를 줄 것이라고 시사한다. 추후에 수행될 이러한 연구 주제들을 통해 순수한 나노물방울 연구가 에어로졸 혹은 미세 먼지 관련 분야에 응용될 수 있는 가능성을 타진해 보려고 한다.

주요어 : 표면장력, 나노물방울, 분자동역학, 톨만 길이, 깁스-톨만-쾨니그-버프 방정식, 밀도함수이론

학 번 : 2009-20398